

NAVAL POSTGRADUATE SCHOOL

Monterey, California



THESIS

An Investigation on Temperature
Fluctuations over Ocean Waves

by

David Marcus Ihle

Thesis Advisor

K. L. Davidson

September 1972

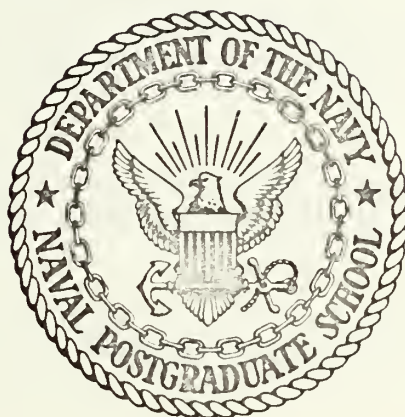
Thesis
I18

Approved for public release; distribution unlimited.

Library
San Jose State University School
San Jose, California 95194

NAVAL POSTGRADUATE SCHOOL

Monterey, California



THESIS

An Investigation on Temperature
Fluctuations over Ocean Waves

by

David Marcus Ihle

Thesis Advisor

K. L. Davidson

September 1972

Approved for public release; distribution unlimited.

An Investigation on Temperature
Fluctuations over Ocean Waves

by

David Marcus Ihle
Lieutenant, United States Navy
B.S., Oklahoma State University, 1962

Submitted in partial fulfillment of the
requirements for the degree of

MASTER OF SCIENCE IN METEOROLOGY

from the
NAVAL POSTGRADUATE SCHOOL
September 1972

11-10-69
U.S. Navy
11-10-69

ABSTRACT

Joint probability distributions and conditional means functions are used to analyze turbulent wind and temperature data obtained over natural ocean waves. The data were collected aboard R/V FLIP during BOMEX 1969.

Stable conditions prevailed during all time periods considered. The emphasis is to use the statistical procedures to describe the wave's influence on the temperature fluctuations at the 8 meter level.

Results are compared with predictions given by potential flow theory. The results consistently demonstrate that waves exert an influence on the temperature fluctuations. In addition, it is observed that under near neutral thermal stratification or prolonged periods of stable thermal stratification the temperature fluctuations approached those expected from potential flow.

TABLE OF CONTENTS

I.	INTRODUCTION -----	9
II.	BACKGROUND -----	12
	A. THEORETICAL APPROACH -----	12
	B. OBSERVATIONAL APPROACH -----	13
III.	DESCRIPTION AND MEASUREMENT OF DATA -----	21
	A. LOCATION OF R/V FLIP -----	21
	B. SENSOR MOUNTING AND INSTRUMENTATION -----	21
IV.	STATISTICAL CONSIDERATIONS AND PROCEDURES -----	26
	A. SUMMARY OF JOINT PROBABILITY DENSITY FUNCTION (JDF)/CONDITIONAL MEAN FUNCTION (CMF) PROCEDURES -----	26
	B. BANDPASS FILTER -----	29
	C. NORMALIZATION OF DATA AND COMPUTATION OF STATISTICS -----	29
	D. JDF/CMF COMPUTATION -----	30
	E. STATISTICAL EDDY PERIOD COMPUTATION -----	30
	F. PHASE AMPLITUDE COMPUTATION -----	30
	G. SUMMARY OF ANALYSIS PROCEDURES -----	32
V.	GENERAL WIND, WAVE, AND THERMAL STRATI- FICATION CONDITIONS -----	33
VI.	PRESENTATION OF RESULTS -----	36
	A. SPECTRAL AND "STATISTICAL EDDY PERIOD" RESULTS -----	36
	B. JDF/CMF PRESENTATION FOR POTENTIAL FLOW CASE	37
	C. PERIOD 1 RESULTS -----	45
	D. PERIOD 2 RESULTS -----	49
	E. PERIOD 3 RESULTS -----	51
	F. PERIOD 4 RESULTS -----	61

VII. CONCLUSION -----	70
APPENDIX - ADDITIONAL JDF/CMF AND PHASE AMPLITUDE RESULTS -----	73
BIBLIOGRAPHY -----	85
INITIAL DISTRIBUTION LIST -----	86
FORM DD 1473 -----	88

LIST OF FIGURES

1.	Waveforms of u , w , T and wT with respect to the ocean waves assuming potential flow theory----	14
2.	$\sigma T/ T_* $ vs c/u_* According to the Monin-Obukhov Similarity Theory -----	17
3.	Arrangements during BOMEX (a) Geographic Position, (b) Sensor Location on Board R/V FLIP -----	22
4.	Temperature system (a) Diagram of the temperature probe, (b) Bridge-amplifier system (constant current) -----	24
5.	Mean wind and wave conditions during BOMEX 69 -----	25
6.	JDF/CMF Array (a) Example of printed JDF/CMF array, (b) Octant and wave amplitude class boundary used for phase amplitude determination --	27
7.	Block diagram of computer steps to produce a smooth JDF/CMF array -----	28
8.	Response curve for inverse transform band-pass filter -----	29
9.	Example of phase amplitude results for potential flow case -----	31
10.	$\sigma T/ T_* $ vs c/u_* For this study compared to values obtained by Volkov (1969) -----	34
11.	Temperature spectra for periods 1, 3 and 4 -----	39
12.	Temperature, \overline{wT} , and wave spectra at (a) beginning and (b) end of period 1 -----	40
13.	Temperature, \overline{wT} , and wave spectra at (a) beginning and (b) end of period 3 -----	41
14.	Temperature, \overline{wT} , and wave spectra at (a) beginning and (b) end of period 4 -----	42
15.	JDF/CMF Patterns associated with potential flow case -----	43
16.	JDF/CMF Results for period 1 subset 1 -----	50
17.	JDF/CMF Results for period 1 subset 2 -----	51

18.	JDF/CMF Results for period 1 subset 3 -----	52
19.	JDF/CMF Results for period 1 subset 4 -----	53
20.	Phase amplitude results for period 1 subset 1(a) small waves, (b) large waves, and (c) all waves -----	54
21.	Phase amplitude results for period 1 subset 2(a) small waves, (b) large waves, and (c) all waves -----	55
22.	Phase amplitude results for period 1 subset 3(a) small waves, (b) large waves, and (c) all waves -----	56
23.	Phase amplitude results for period 1 subset 4(a) small waves, (b) large waves, and (c) all waves -----	57
24.	JDF/CMF Results for period 2 subset 1 -----	60
25.	JDF/CMF Results for period 2 subset 2 -----	61
26.	Phase amplitude results for period 2 subset 1 (a) small waves, (b) large waves, and (c) all waves -----	62
27.	Phase amplitude results for period 2 subset 2 (a) small waves, (b) large waves, and (c) all waves -----	63
28.	JDF/CMF Results for period 3 subset 1 (a) small waves, (b) large waves, and (c) all waves -----	65
29.	Phase amplitude results for period 3 subset 1(a) small waves, (b) large waves, and (c) all waves -----	66
30.	JDF/CMF Results for period 4 subset 1 -----	68
31.	Phase amplitude results for period 4 subset 1 (a) small waves, (b) large waves, and (c) all waves -----	69
32.	JDF/CMF Results for period 2 subset 3 -----	73
33.	JDF/CMF Results for period 2 subset 4 -----	74
34.	Phase amplitude results for period 2 subset 3 (a) small waves, (b) large waves, and (c) all waves -----	75

35.	Phase amplitude results for period 2 subset 4 (a) small waves, (b) large waves, and (c) all waves -----	76
36.	JDF/CMF Results for period 3 subset 2 -----	77
37.	JDF/CMF Results for period 3 subset 3 -----	78
38.	Phase amplitude results for period 3 subset 2 (a) small waves, (b) large waves, and (c) all waves -----	79
39.	Phase amplitude results for period 3 subset 3 (a) small waves, (b) large waves, and (c) all waves -----	80
40.	JDF/CMF Results for period 4 subset 2 -----	81
41.	JDF/CMF Results for period 4 subset 3 -----	82
42.	Phase amplitude results for period 4 subset 2 (a) small waves, (b) large waves, and (c) all waves -----	83
43.	Phase amplitude results for period 4 subset 3 (a) small waves, (b) large waves, and (c) all waves -----	84

ACKNOWLEDGEMENTS

The author wishes to take this opportunity to express his appreciation to his advisor, Professor K. L. Davidson, for his support, advice, and guidance throughout this research.

Appreciation is also expressed to Professor N. E. Boston for his careful review of the manuscript and useful suggestions, and to Sharon Raney for assistance with computer tape conversions.

To the W. R. Church Computer Facility of the Naval Postgraduate School, thank you for the free use of the IBM 360 Computer. In particular, a heartfelt thanks to the evening operators Chris Bertwell, Edwin Donnellan, and Parker Thomas.

The research was made possible by the Office of Naval Research through Contract N00014-67-A-0181-005 with the University of Michigan and Task NR 083-265 with the Naval Postgraduate School.

The manuscript was typed by Miss Marion Marks.

Finally, and most importantly, to my wife Sharon for her love, understanding, patience, and the typing of the first drafts and to my son Marcus who had only a part-time father for two years, thank you.

I. INTRODUCTION

Turbulent and wave induced temperature fluctuations over ocean waves may be described by theoretical models or inferred from observations. These descriptions are necessary to develop an understanding of a wide class of applied problems which require a knowledge of sensible heat transfer and the nature of temperature fluctuations.

Vertical turbulent transfers of both sensible and latent heat in the boundary layer are influenced by modifications induced in the overlying air mass by the surfaces below. Most present theories and procedures for estimating these transfers are based to a large extent on empirical formulae developed from data obtained over land. These include assumed profiles for the mean wind, temperature and humidity.

However, recent theoretical and observational studies that will be described in the background section suggest that transfer processes over ocean waves may be influenced, and not necessarily in a simple manner, by the waves themselves. Therefore, one cannot assume that phenomena which are fairly well understood over land are also understood over water until the wave's influences are adequately determined.

One applied problem in which a better description of the temperature fluctuations over waves is required is the optical (laser) propagation problem. These studies require a knowledge of the refractive index in order to predict the path and the scintillation of optical wave propagation.

Temperature fluctuation would influence this index and thereby optical wave propagation. Optical wave propagation is presently based on stability parameters which ignore the influence of waves.

The purpose of this study is to examine turbulent features of the temperature structure over natural ocean waves. The observational data were obtained aboard R/V FLIP (Floating Instrument Platform) during BOMEX (Barbados Oceanographic and Meteorological Experiment) during the period 19 to 28 May 1969. The data examined are from simultaneous measurements of velocity components (u, v, w), temperature (T) at fixed levels above mean sea level and wave height (η).

The analyses methods used in this study are the same as those in an investigation of velocity fluctuations over waves by Davidson and Frank (1973). However, temperature fluctuations are the parameters of interest in this study whereas the velocity fluctuations were considered in the referenced study. Statistical procedures applied in these analyses are joint probability density function and conditional mean function. The former will be referred to as (JDF) and the latter as (CMF) in the remainder of this thesis. This study was the first application of the JDF/CMF analysis to temperature data over ocean waves. Results will be discussed in relation to observational studies by Volkov (1969), Phelps and Pond (1971) and Pond et al. (1971).

In addition to the JDF/CMF statistical procedures this study will include spectral results. Thompson (1972) s

conducted a study of momentum transfer features using the same statistical procedures and the same time periods.

II. BACKGROUND

A study of boundary layer wave induced fluctuations requires some sort of physical theory connecting observed properties to those we wish to infer. This physical theory may be obtained by developing a model which gives realistic results or by observing real data and describing what has occurred. The results of such studies will frequently allow inferences of properties other than those that are measurable directly by instruments. This background discussion will first consider some papers presenting theoretical approaches and then review recent attempts to use real data.

A. THEORETICAL APPROACH

With respect to theoretical predictions Stewart (1969) has suggested that with a stable thermal stratification the study of turbulent fluctuations is complicated by the fact that motion due to both turbulence and internal gravity waves is present and the aspects we would like to infer are totally different for each kind of motion. In addition to the existence of two different types of fluctuations, there is a nonlinear coupling between waves and turbulence. Stewart (1969), while looking for a tracer of turbulent motion, stated that:

"... the waves are capable of transporting momentum but they are not capable of transporting passive scalars per se."

Therefore, he suggests using a scalar tracer transport in order to see turbulent effects. This in effect implies that

a scalar such as temperature could be predicted by potential flow theory. Velocity, temperature and heat flux streamlines shown in Figure 1 are those that would occur under stable temperature stratification and potential flow. This concept of the coupling between a scalar temperature field over a natural wave field is in contrast to that presented by Volkov (1969) which will be reviewed later in this text.

In a theoretical study, Witting (1972) considered an irrotational, plane, periodic, linear progressive wave model to study the variation of surface temperature induced by waves and thereby make it possible to estimate the amount of phase shift away from potential flow. He concluded that (1) when the wave period is sufficiently small (≤ 3 sec) the amplitude of the wave induced temperature fluctuation is proportional to the wave amplitude and to the square root of the wave period, (2) surface temperature maxima lead wave crests by one-eighth of a period when the average surface temperature is less than the bulk water temperature and (3) surface temperature minima lead wave crests by one-eighth of a period when the average surface temperature exceeds that of the water below. This theoretical study then recognizes wave induced fluctuations in the scalar temperature field and a deviation from potential flow.

B. OBSERVATIONAL APPROACH

Since theoretical studies do not agree, attention is directed toward observational studies. Phelps and Pond (1971)

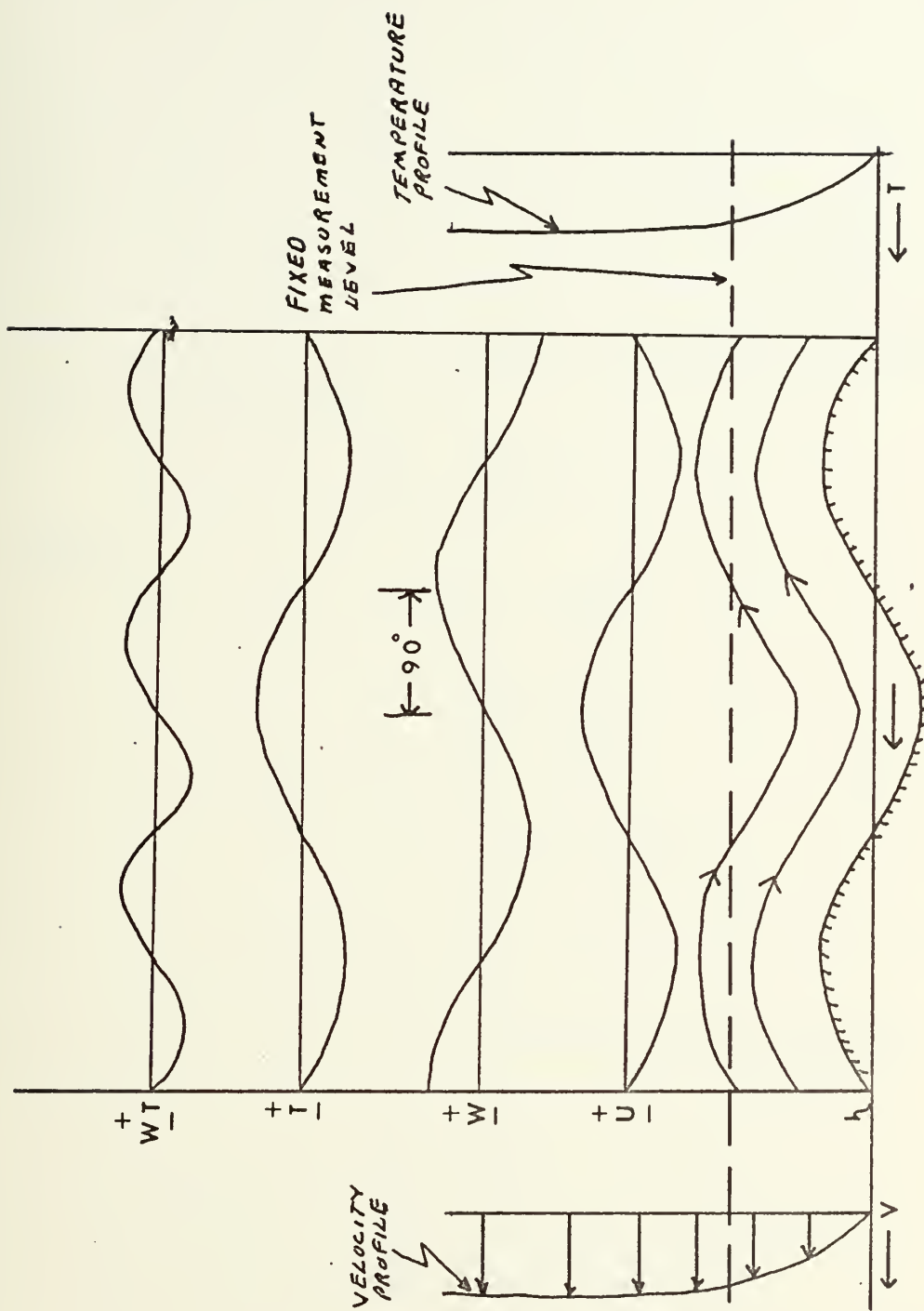


Figure 1. Waveforms of u , w , T and WT with respect to the ocean waves assuming potential flow theory.

and Pond et al. (1971). examined data obtained aboard R/V FLIP during BOMEX 1969. However, in their study wave motion was not measured and no recognition is given to wave induced temperature fluctuations. According to similarity theory predictions, the intensities of velocity and temperature fluctuations should depend only on the wind speed, the roughness of the underlying surface and the thermal stratification. In the case of temperature fluctuations, this dependence can be expressed as

$$\frac{\sigma T}{T_*} = f(Z/L)$$

where

$$T_* = \frac{1}{\kappa} \cdot \frac{\overline{wT'}}{u_*}$$

$$T' = (T - \overline{T})^{1/2}$$

$$u_* = (-\overline{uw})^{1/2}$$

$$L = -\overline{T} u_*^3 / \kappa g \overline{wT'}$$

$$\kappa = \text{von Karman's Constant}$$

$$w' = w - \overline{w}$$

$$w = \text{observed vertical motion}$$

$$\overline{w} = \text{mean vertical motion}$$

$$T' = T - \overline{T}$$

$$T = \text{observed temperature}$$

$$\overline{T} = \text{mean temperature}$$

$$Z = \text{height above mean sea level}$$

Therefore, the ratio $\sigma T/T_*$ should depend only on Z/L . Such a dependence has been verified in numerous overland

experiments. In particular, the ratio has been observed to have a value of approximately 1 in near neutral conditions.

Phelps and Pond (1971) observed agreement between this $\sigma T/T_*$ results and the similarity theory predictions with respect to Z/L . However, they also observed that $\sigma T/T_*$ varied as c/u_* , where c corresponds to the phase speed of the predominant surface wave. Kitaygorodskiy (1969) and Volkov (1969) initially suggested that such a relationship should exist. Because $\sigma T/T_*$ is inversely proportional to the efficiency of the turbulent flow to transport sensible heat, the latter findings imply that over a wave surface there are considerable temperature fluctuations which are not associated with heat transfer. The latter, of course, was suggested by Stewart (1969) with respect to wave motion within a thermally stratified layer.

The observed relationship between $\sigma T/T_*$ and c/u_* appears in Figure 2. The curves mean square deviations are those constructed by Volkov (1969). This suggested curve will be compared later to results obtained in this study.

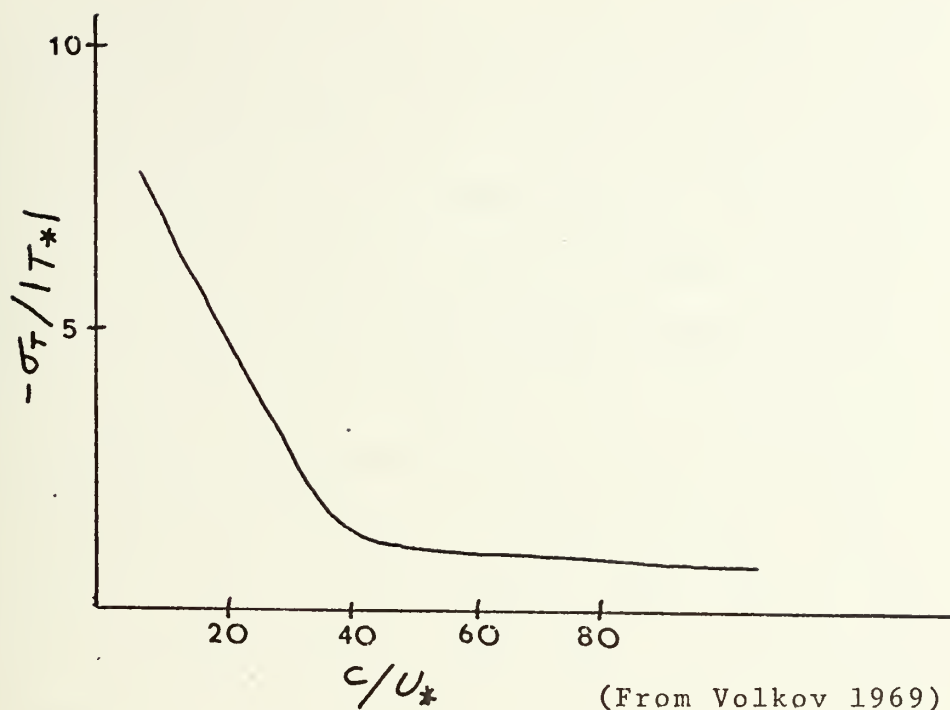


Figure 2. $\sigma_T/|T_*|$ vs c/u_* According to Monin Obukhov Similarity Theory.

Phelps and Pond (1971) used data similar to Pond et al. (1971) to describe the similarities and differences between temperature, humidity, and velocity fluctuations. They found that over a wide frequency range the temperature waveform leads the vertical velocity and humidity waveform by 20-40 degrees, but they attributed this to instrument effects and R/V FLIP's motion. Again it should be noted that no wave data were available for their experiment. They also concluded that humidity and vertical velocity are basically in phase. No humidity data were available for the present study.

In another observational study Volkov (1969) reduced western Mediterranean data according to similarity theory in order to compare characteristics of turbulence in th

atmospheric boundary layer above an agitated sea surface with measurements in the boundary layer above dry land. He states that the main difficulty in interpreting atmospheric measurements above the sea is the presence of a mobile fluid air-water interface which has an irregular variation as a result of wind action and airflow-wave feedback processes. The feedback is due to the surface waves disturbing the airflow around them and forming waves in the air which interact with the velocity gradient of the basic flow. The wave induced motion in the air flow causes some energy to be transferred from the basic flow to the waves. These processes also effect the fluctuation of a scalar such as temperature or moisture. In particular Volkov (1969) suggests that an observed temperature (T) above a wave surface should be made up of the mean temperature ($\bar{T}(z)$), turbulent fluctuations ($T'(x,y,z,t)$) and wave induced fluctuations ($T''(x,z)$). Therefore:

$$T = \bar{T}(z) = T''(x,z) + T'(x,y,z,t)$$

Therefore, of special significance in studying the structure of turbulence in the atmospheric boundary layer above the agitated sea surface are measurements of the fluctuations of velocity (u,w), temperature (T) and emphatically, wave height (η). It should be noted that Phelps and Pond (1971) and Pond et al. (1971) did not have simultaneous measurements of wave height included in their data.

By the use of spectral analysis Volkov (1969) was able to conclude that the spectra of fluctuations above the

agitated sea surface are due to two types. One type of fluctuation corresponds to those smaller than the characteristic scales of sea swell and is close to the corresponding interval of the turbulence spectrum for the air layer above land. The other type corresponds to fluctuations of the order of the characteristic size of the surface waves and is typified by the superposition of wave disturbances on the random turbulent field of the fluctuations. The latter type was shown in Figure 1 as potential flow.

Davidson and Safley (1973) in another observational study described the occurrence of micro-thermals, large positive temperature fluctuations, and provided arguments supporting the concept of wave influence on micro-thermals. A review of the literature associated with wind-wave coupling was provided by Davidson and Safley (1972) who strongly suggest that the wave's influence could contribute to micro-thermal formation in the case of two proposed mechanisms. These mechanisms were the existence of wave-related motion in airflow which is too organized to be viewed as turbulent and instantaneous distortions of the wind shear over different phases of the surface wave. Velocity spectral results from a Lake Michigan study were used to show that the waves could have played a role in the observed micro-thermal phenomena due to wave related vortices in the mean shear. However, large thermal instability associated with the periods used in the referenced study did not allow a detail description of the precise role of the waves.

On the basis of the results of Witting (1972), Volkov (1969) and Davidson and Safley (1972) just described, there is reason to expect that the wave surface has a considerable influence on all of the statistical characteristics of turbulence in the near surface layer. Volkov (1969) states this fact in the following manner:

"We therefore succeed in finding some typical features and regularities of this influence by the complex method of investigating the processes of interaction between the atmospheric boundary layer and the agitated sea surface."

The present study is an attempt to describe the above processes through the use of actual data and statistical procedures to test concepts put forth by Volkov (1969) whose results were obtained by semi-empirical arguments.

III. DESCRIPTION AND MEASUREMENT OF DATA

A. LOCATION OF R/V FLIP

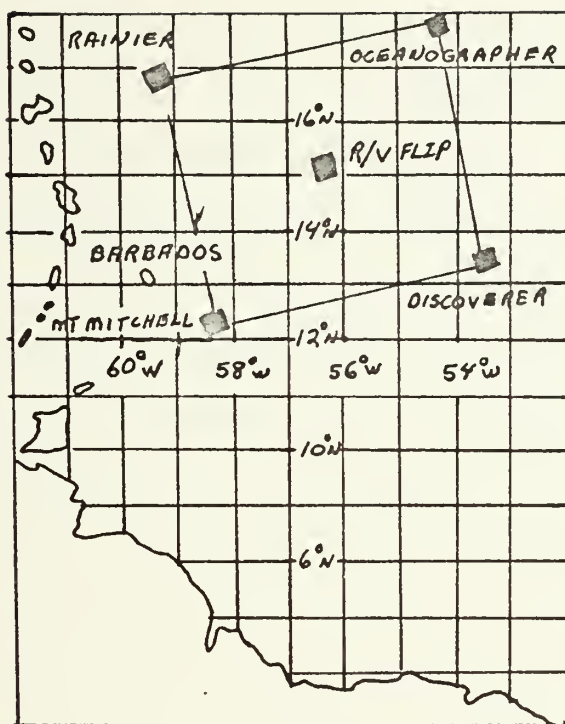
The data were from measurements taken by University of Michigan personnel during the BOMEX experiment of 1969. The data consisted of velocity, temperature, vertical motion and wave height measurements at three and eight meter levels. The data examined were from 19, 26, and 28 May 1969. During this period R/V FLIP was located northeast of Barbados, Figure 3A.

FLIP's position into the wind was held by a tug attached with a bridle and approximately 800 meters of line. The tug then steamed slowly downwind.

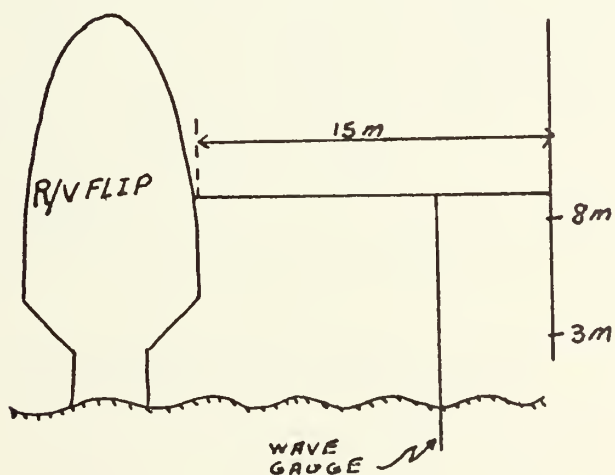
B. SENSOR MOUNTING AND INSTRUMENTATION

Instrument location relative to R/V FLIP is shown in Figure 3B. As indicated, all sensors were mounted on the vertical mast.

Temperature fluctuations were measured by a resistance thermometer, Figure 4A. The sensor consisted of a 30 ohm, 0.00015 inch diameter tungsten wire, 0.16 inches long as part of a constant-current circuit with a small filament current (about 2ma) to serve as a resistance thermometer. The frequency response of the system is determined primarily by the thermal inertia.



(A) (from Portman et al. 1970)



(B)

Figure 3. Arrangements during BOMEX (A) Geographic position, (B) Sensor location on board R/V FLIP.

A block diagram of the bridge circuit is shown in Figure 4B.¹ An unbalance of the bridge is caused by temperature and thereby a sensor resistance change.

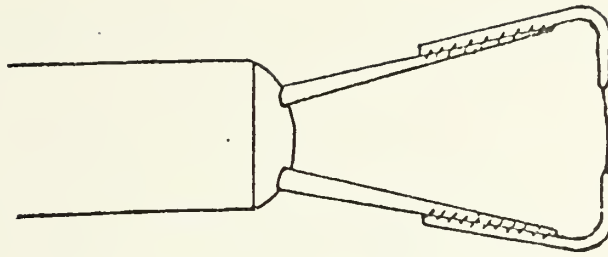
System noise and sensitivity restricted spectral description of temperature to frequencies below 20 Hz. Since sensible heat flux is associated with frequencies below 10 Hz (Deacon 1959), the response was sufficient for this aspect of the interpretations. Furthermore, of particular interest is the frequency response near the frequency of the dominate surface wave, approximately 0.1 Hz.

Velocity measurements were made with a constant-temperature hot-film anemometer² system using three sensor probes. A discussion of this equipment is provided by Portman et al. (1970).

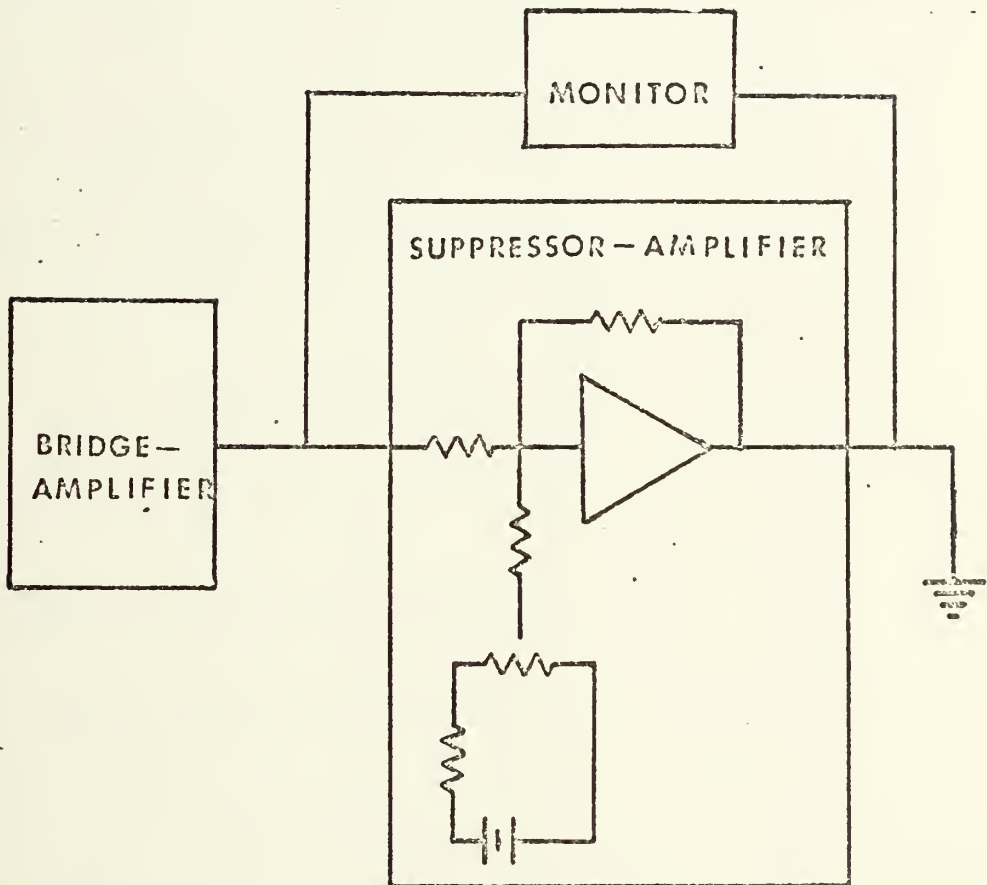
Visual estimates of wave height and 10 meter wind speed are shown in Figure 5. All periods considered are characterized by stable thermal stratification with swell type waves propagating through the area.

¹Flow Corporation System, Series 900

²Thermo-System Incorporation, Model 1054B



(A)



(B) (from Davidson 1970)

Figure 4. Temperature system (A) Diagram of the temperature probe, (B) Bridge-amplifier system (constant current).

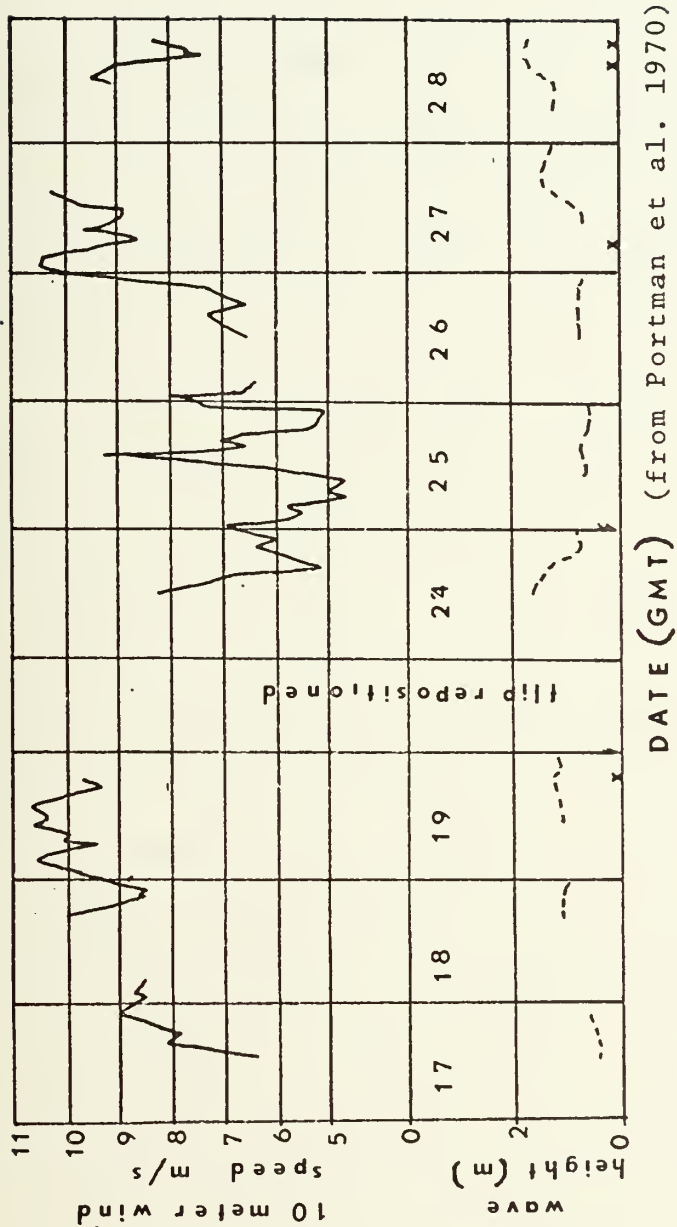


Figure 5. Wind and wave conditions during BOMEX 69
 X period used for this study
visual estimate of wave heights.

IV. STATISTICAL CONSIDERATIONS AND PROCEDURES

A. SUMMARY OF JDF/CMF PROCEDURES

Joint probability density function (JDF) and conditional mean function (CMF) statistical procedures used in this study are based on descriptions by Holland (1968, 1972). The same procedures were applied by Frank (1971), Davidson and Frank (1973) and Thompson (1972) to small scale fluctuations over waves.

A JDF allows simultaneously observed pairs of values to be represented by contours on a two dimensional array. A trivariate statistical relationship is obtained by computing a conditional mean of a third variable as a function, CMF, of the two independent variables contributing to the JDF. These statistics are determined for variables that are normalized by their standard deviation.

A JDF/CMF array appears in Figure 6A in which both the ordinate and abscissa are given in standard deviation (σ) units. The array is centered on the mean value, which is zero, of the two JDF variables. The bottom number on each cell represents the JDF (the probability $\times 10^3$ of the joint occurrence of the pair). A nine point smoother was used to remove the perturbations viewed as being physically and statistically insignificant. Statistical procedures necessary to obtain final JDF/CMF results are shown in Figure 7 and will be described briefly in the following paragraphs. A complete discussion of the theory associated with these

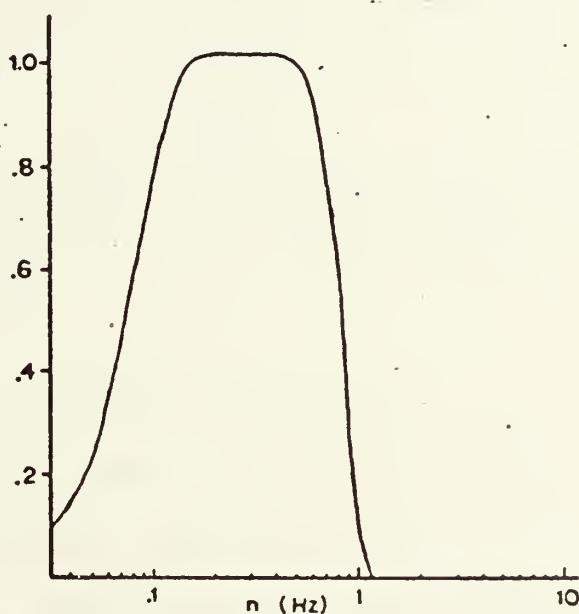
NORMALIZATION AND COMPUTATION OF STATISTICS FOR THE VARIABLES	1
BANDPASS FILTERING	2
COMPUTATION OF JDF/CMF, APPLICATION OF A 9 POINT SMOOTHER, COMPUTATION OF STATISTICAL EDDY PERIODS, AND PRINT OUT OF ARRAY	3
COMPUTATION OF PHASE AMPLITUDE INFORMATION USING PHASE ANGLE	4
CLASSIFY INTO LARGE AND SMALL AMPLITUDE WAVES	5
PLOTTING OF JDF/CMF VARIABLES AND PHASE AMPLITUDE	6

Figure 7. Block diagram of computer steps to produce a smooth JDF/CMF array.

procedures was presented by Holland (1968, 1972), and a more complete discussion of its application in this study is provided by Frank (1971).

B. BANDPASS FILTER

The bandpass filter, shown as step 1, was an inverse transform filter. This was applied to isolate the significant frequency band (0.1 Hz to 0.8 Hz) associated with the ocean waves. Its response curve is shown in Figure 8.



(from Frank 1971)

Figure 8. Response curve for inverse transform band-pass filter.

C. NORMALIZATION OF DATA AND COMPUTATION OF STATISTICS

Normalization of data, shown as step 2 in the flow diagram, was performed as described in subsection A.

D. JDF/CMF COMPUTATION

The JDF/CMF array, shown as step 3 in Figure 7, is described in the beginning of this section. Procedures for this were described by Frank (1971) and Thompson (1972).

E. STATISTICAL EDDY PERIOD COMPUTATION

The "statistical eddy period" computed in step 3, was suggested by Holland (1968, 1972) as an approach to reveal if the amplitude of the dependent variable such as temperature varies nonlinearly with the amplitude of the independent variable such as wave height. Holland defined a "statistical eddy period" $\tau_o = 2\pi \frac{\sigma_y}{\sigma_{\dot{y}}}$ for any fluctuating meteorological variable y . σ_y is the standard deviation of the meteorological variable and $\sigma_{\dot{y}}$ is its derivative.

F. PHASE AMPLITUDE COMPUTATION

Phase amplitude computation, shown as step 4 in the flow diagram, was determined from a JDF coordinate system with (η) as ordinate and its derivative $(\dot{\eta})$ as the abscissa. This allowed presentation of the phase of the variable with respect to the wave. The phase angle was defined by an angle measured (by octants) counterclockwise (CCW) from the horizontal axes in the $(\dot{\eta}, \eta)$ coordinate system. This is shown in Figure 6B. A complete discussion of this may be found in Holland (1968, 1972).

The phase amplitude procedures outlined in the above references were performed with respect to the waves for the

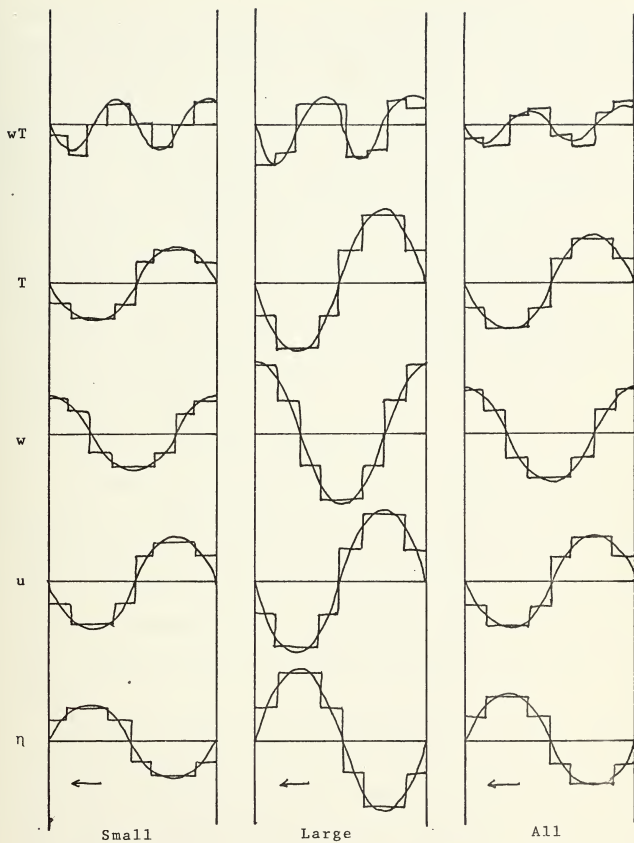


Figure 9. Example of phase amplitude results for potential flow case.

variables u , w , T and wT . Prior to summarizing by octants and plotting, the results were separated into wave amplitude classes defined by regions on the JDF array. Three classes were considered, those being small amplitude (less than 1.5σ), large amplitude (greater than 1.5σ) and the sum of the first two. This yielded, therefore, phase relationships with respect to small, large and all surface waves.

Summarized phase amplitude results for each octant, as described in Figure 6B, are shown by horizontal bars that appear in Figure 9. Smooth lines were drawn through each set of horizontal bars such that areas above and below the resulting curves were equal.

G. SUMMARY OF ANALYSIS PROCEDURES

The previous discussion of JDF/CMF analysis procedures indicate that joint probability results are well suited for identification of fluctuations associated with waves. This type of result is particularly useful because it will reveal non-linear properties in fluctuations. These properties were alluded to by Volkov (1969) and Davidson and Frank (1973).

As will be shown in the presentation of results, some of the most significant interpretations will be with respect to the phase amplitude relations. These results do not represent phase amplitude information as revealed by simple linear expansion of the fluctuations, i.e. spectral analysis, but rather the actual nonlinear average fluctuations over different portions of the average wave.

V. GENERAL WIND, WAVE, AND THERMAL CONDITIONS

Data from four separate measurement periods were considered. These periods were 19 May and 27 May and two on 28 May 1969. They will be referred to as periods 1 through 4 respectively in the following discussion. The times for each period appear in Table 1 and Figure 5A along with information on the mean ten meter wind, the significant wave height, the heat flux (H) and Z/L.

Wave histories in Figure 5A indicate that equilibrium conditions prevail with respect to the waves during all periods. Sea conditions were generally dominated by swell. Period 2 had the lowest significant wave height, 1.3 meters, while the other three periods had significant wave heights of about 2.6 meters. The wind speed at the 8 meter level ranged from 9.5 meters/second for period 4 to 11.8 meters/second for period 2.

The existence of equilibrium conditions with respect to atmospheric and sea conditions for all periods is evident, perhaps, by the fact that the relationship between $\sigma T/T_*$ and c/u_* are comparable to those observed by Volkov (1969). $\sigma T/T_*$ vs c/u_* results from those data are along the horizontal section of Volkov's curve, Figure 10. Volkov (1969) has suggested that this range of values corresponds to conditions with surge or nondeveloping sea. The curve shown in Figure 10 is a replot of Figure 2.

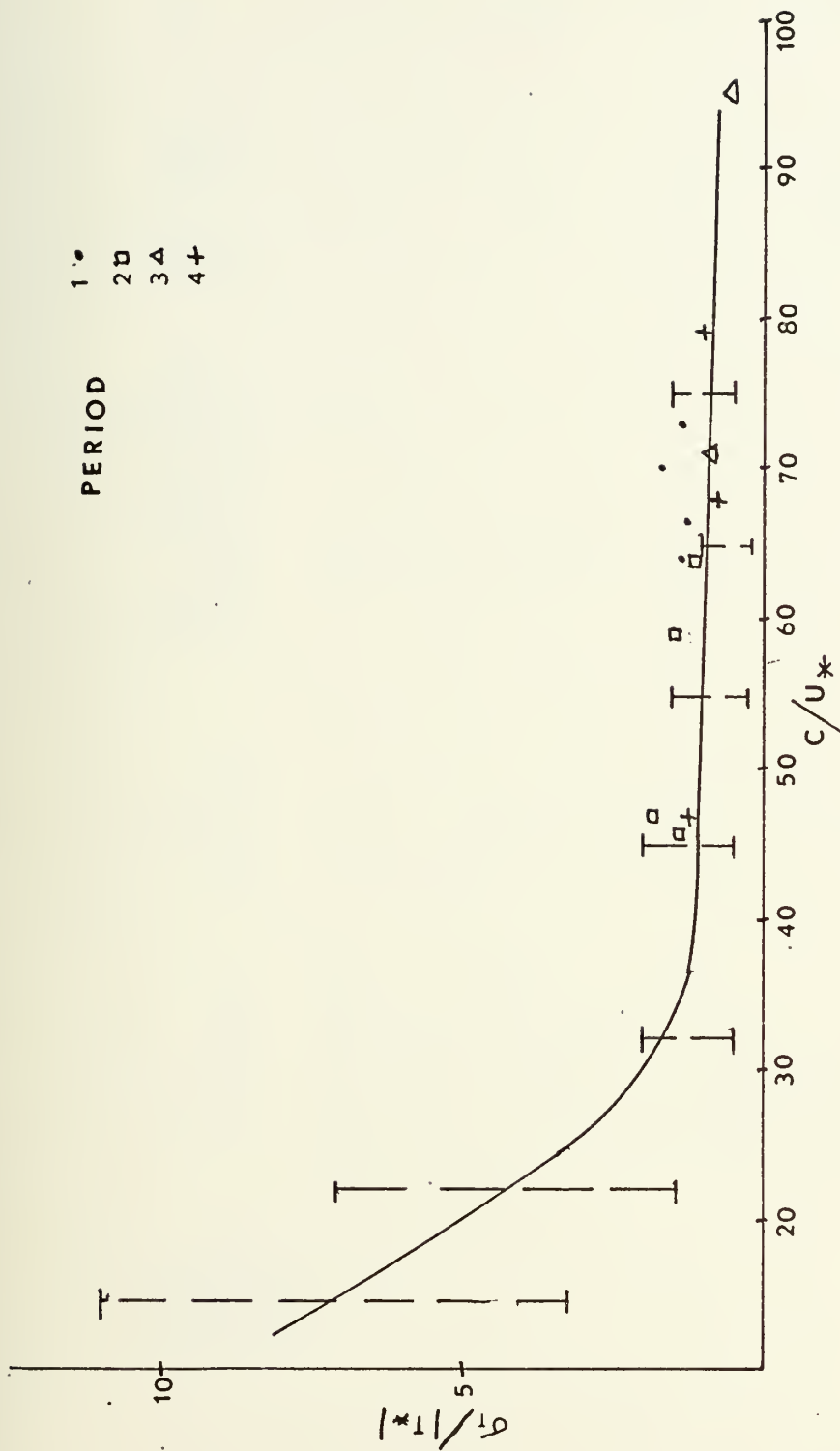


Figure 10. $|T|/|T^*|$ vs c/u^* . For this study compared to values obtained by Volkov (1969).

TABLE 1. General data for the periods analyzed.

PERIOD	NUMBER OF SUBSETS (20 min each)	DATE TIME (GMT)	LEVEL (METERS)	AVG. WIND (MPS) SIGNIFICANT WAVE HEIGHT (METERS)	HEAT FLUX (CAL/CM ² / SEC x 10 ⁴)	Z/L
1	4	19 May 1969 1613-1735	8	10.1 2.8	-1.9	.10
2	4	27 May 1969 0311-0435	8	11.8 1.3	-1.7	.03
3	3	28 May 1969 1754-1916	3	11.0	-2.57	.12
4	3	28 May 1969 2028-2150	8	9.5 2.6	-2.87	.12

VI. PRESENTATION OF RESULTS

A. SPECTRAL AND "STATISTICAL EDDY PERIOD" RESULTS

Temperature spectra for periods 1, 3 and 4 appear in the log-log format of Figure 11. The spectral slope on these plots at high frequencies approaches a $-5/3$ value for all three periods. The $-5/3$ slope is expected for the inertial subrange of a passive scalar.

Pairs of temperature, wT , and wave spectra for periods 1, 3 and 4 are presented in linear-log profiles in Figure 12, 13 and 14. The left side of each Figure is the spectrum at the beginning of each period while the right side is the spectrum occurring near the end.

The most significant characteristic of these spectra is the absence of any noticeable peak in the temperature spectra at the predominant frequency of the wave. Therefore, from an examination of spectra alone it might be mistakenly stated that ocean waves do not influence a passive scalar such as temperature. However, statistical results will be presented to show that temperature fluctuations are indeed influenced by wave motion below.

Spectral results as presented above were not available for period 2.

The "statistical eddy period" was computed as described in section 4 and the results are shown in Table 2. The statistical eddy period for the temperature waveform is always less than that of the ocean wave. This strongly

suggests that potential flow theory will not accurately predict the air sea coupling in the boundary layer.

B. JDF/CMF PRESENTATION FOR POTENTIAL FLOW CASE

The principal comparisons in the discussion of results will be with respect to potential flow theory. These features are based on simple vertical displacement of a thermally stratified air column by the underlying progressive waves. If potential flow theory properly describes the coupling of the air column to the waves, then fluctuations in temperature (T), velocity (u), vertical motion (w) and heat flux (wT) observed by a fixed sensor would appear as shown in Table 1. JDF/CMF results would be those appearing in Figure 15 and phase amplitude results would be those appearing in Figure 9.

A general description of the JDF patterns for potential flow case follows:

1. Uniform circles; 90° phase shift between JDF variables
2. Ellipse; orientated 135° - 315° , JDF variables are in phase
3. Ellipse; orientated 45° - 215° , 180° phase shift in JDF variables.

Dashed lines in all JDF/CMF results correspond to the zero isoline of the CMF. The orientation of various CMF patterns in each panel, as shown in Figure 15, is examined closely in the following interpretations.

TABLE 2. Statistical Eddy Periods.

Period	Subset	$\tau_{WT}(\text{sec})$	$\tau_T(\text{sec})$	$\tau_\eta(\text{sec})$
1	1	2.5	2.7	5.5
	2	2.2	2.7	5.5
	3	2.3	2.8	5.4
	4	2.3	2.8	5.6
2	1	2.2	2.8	4.8
	2	2.3	2.8	4.9
	3	2.3	2.7	4.7
	4	2.3	2.7	4.7
3	1	2.3	2.7	5.5
	2	2.4	2.7	5.8
	3	2.3	2.7	5.6
	4	2.3	2.7	5.8
4	1	2.3	2.7	5.4
	2	2.3	2.7	5.4
	3	2.3	2.7	5.4
	4	2.3	2.7	5.4

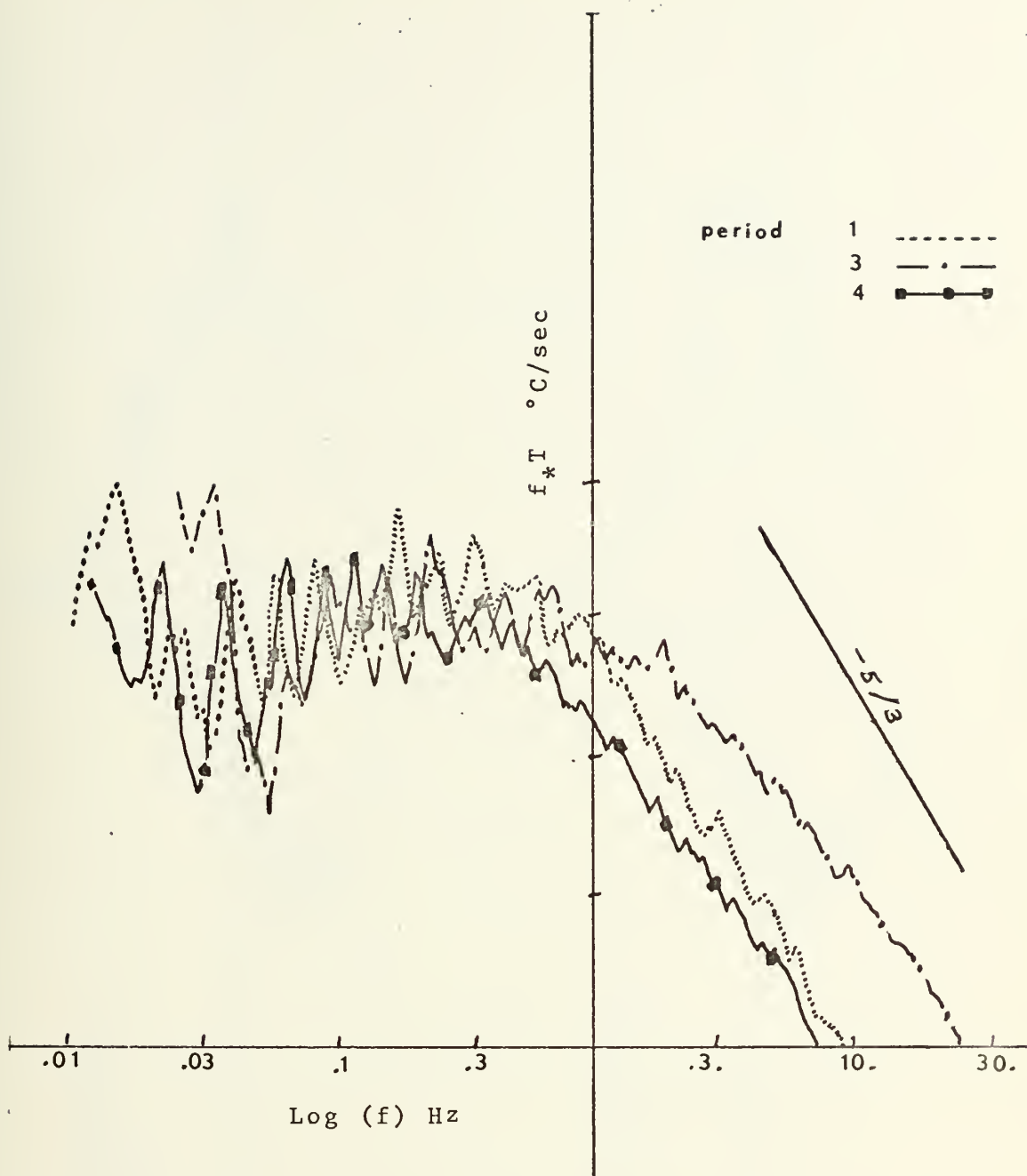


Figure 11. Temperature spectra for periods 1, 3 and 4.

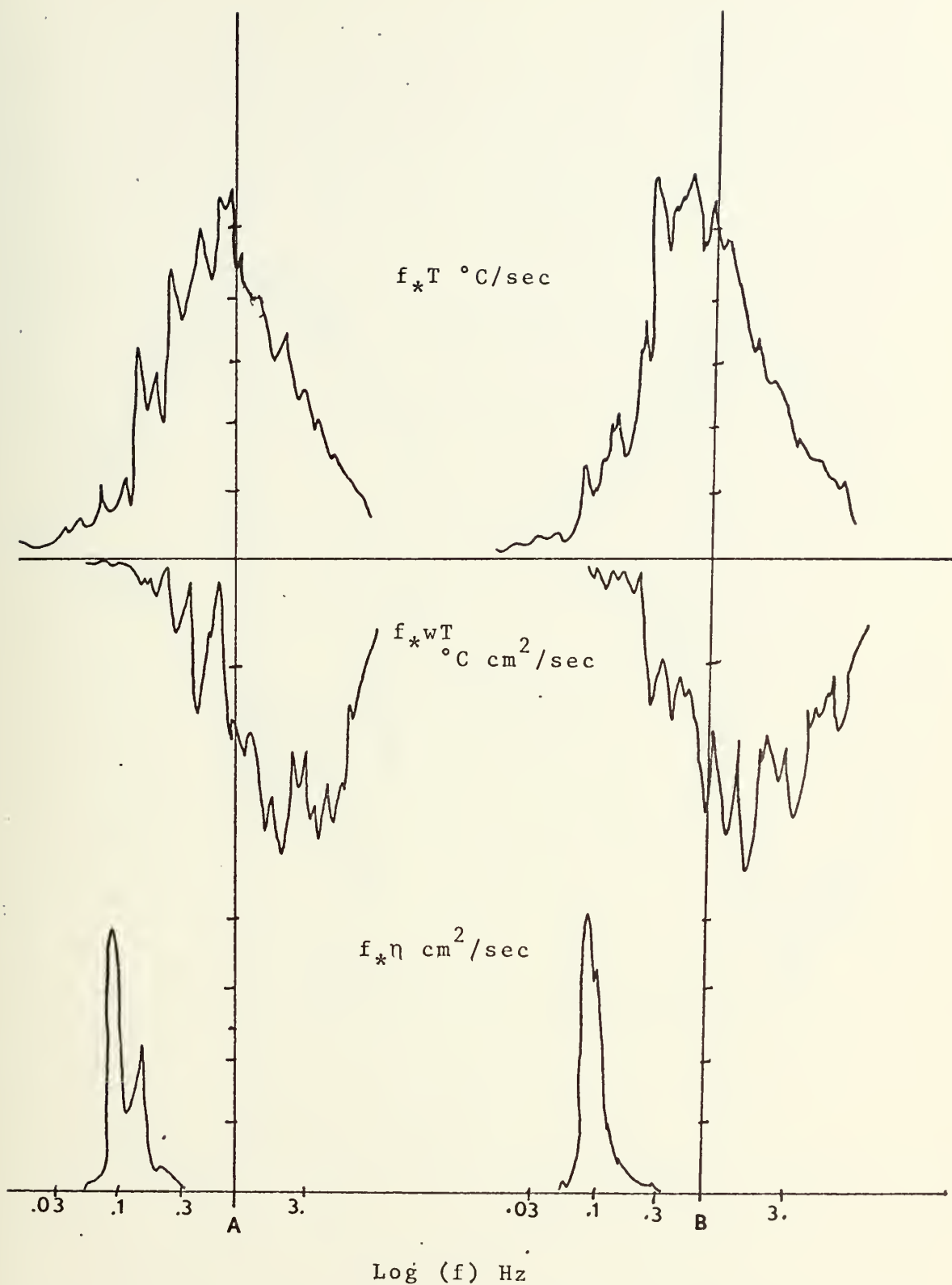


Figure 12. Temperature, \overline{wT} , and wave spectra at (a) beginning and (b) end of period 1.

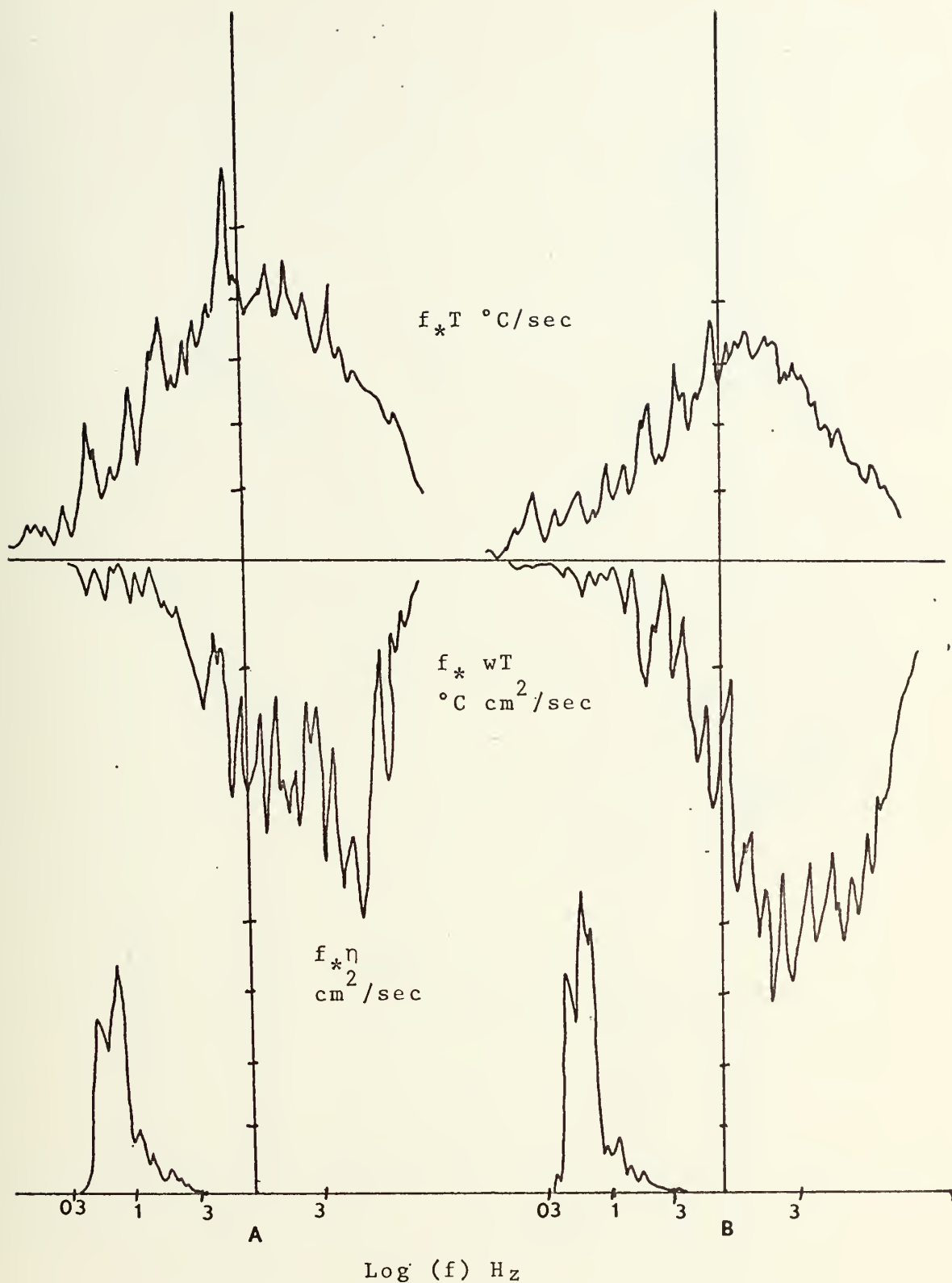


Figure 13. Temperature, \overline{wT} , and wave spectra at (a) beginning and (b) end of period 3.

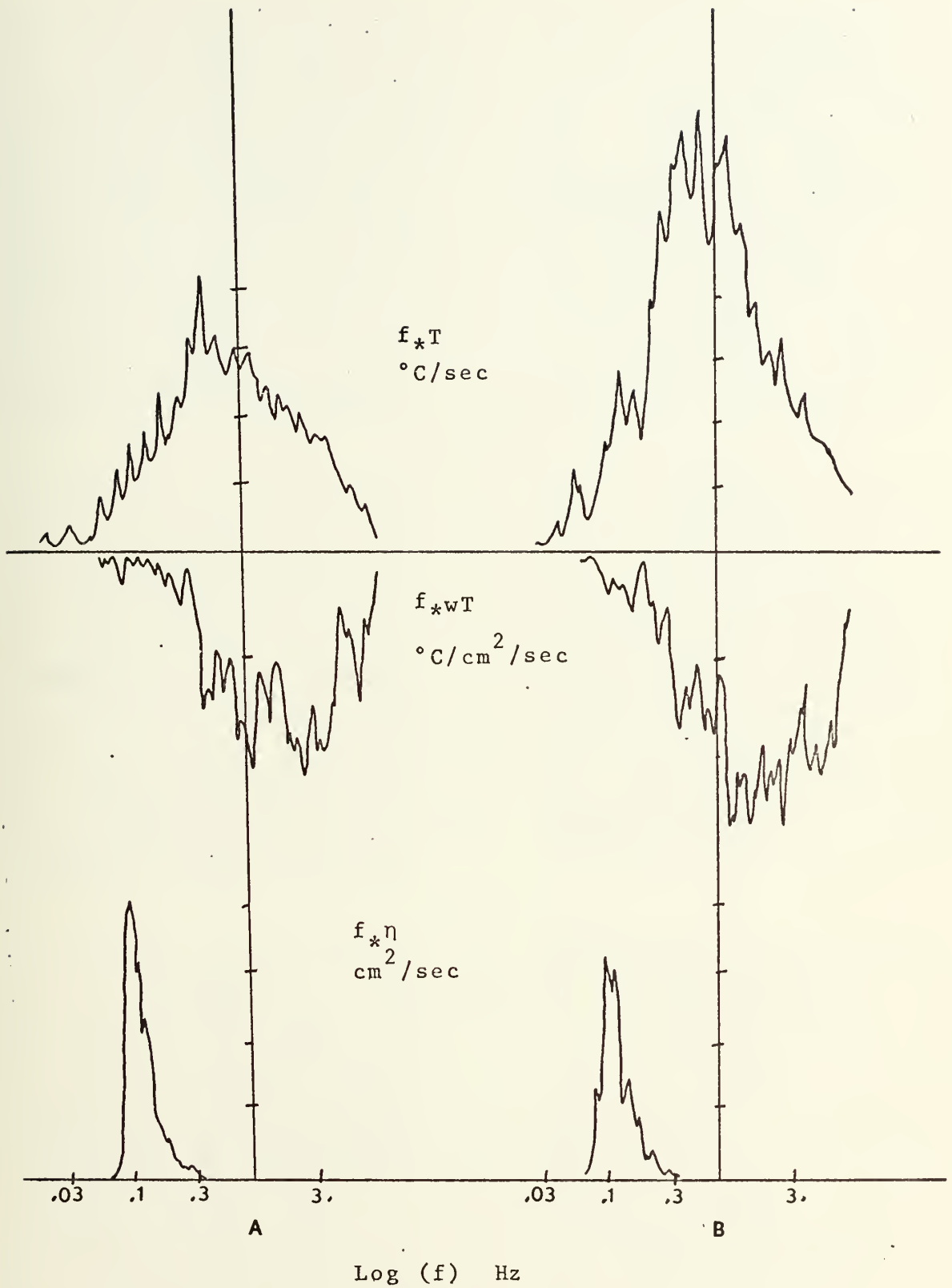


Figure 14. Temperature, \overline{wT} , and wave spectra at (a) beginning and (b) end of period 4.

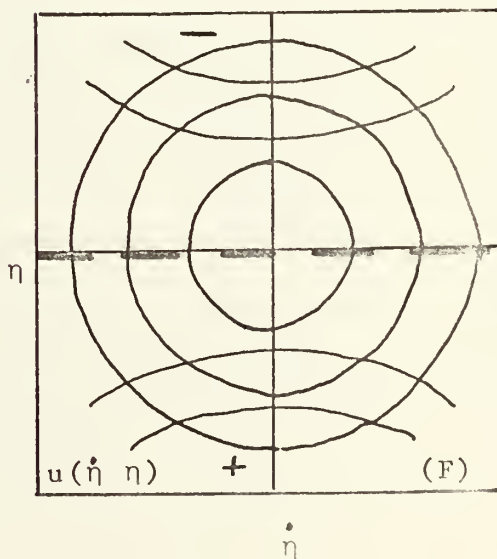
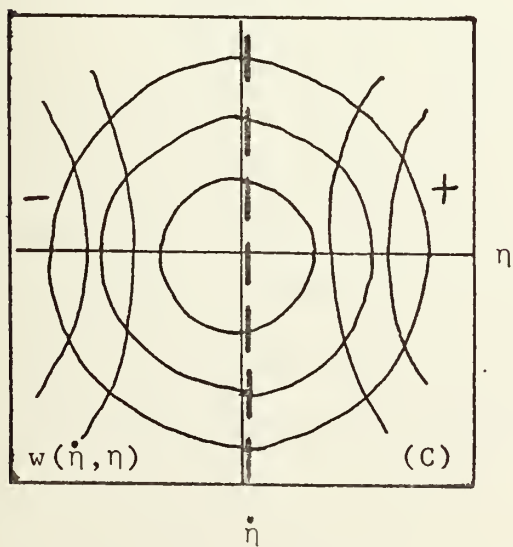
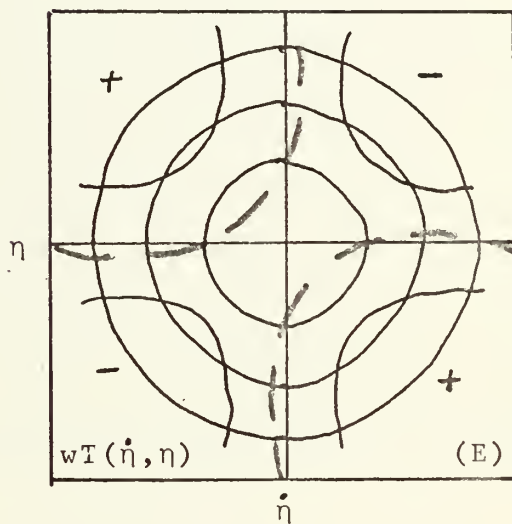
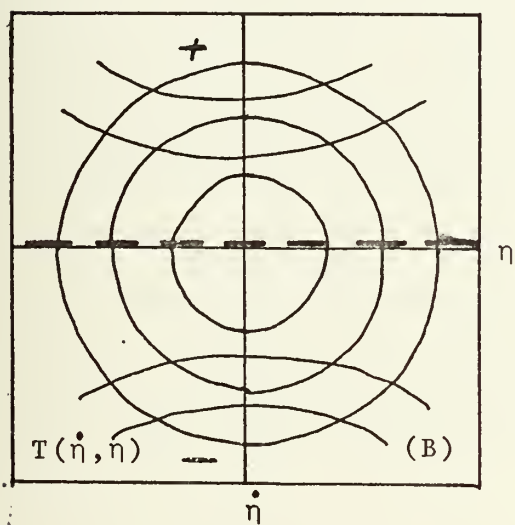
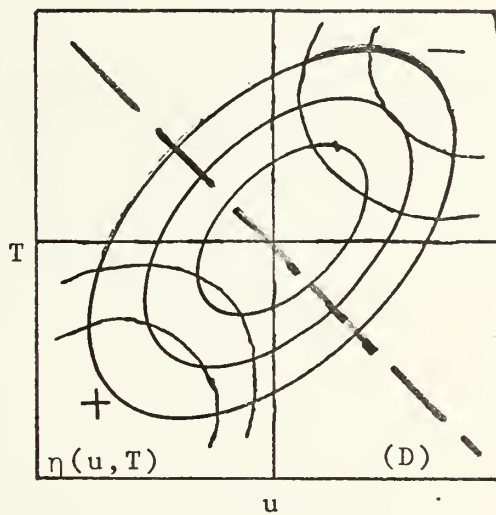
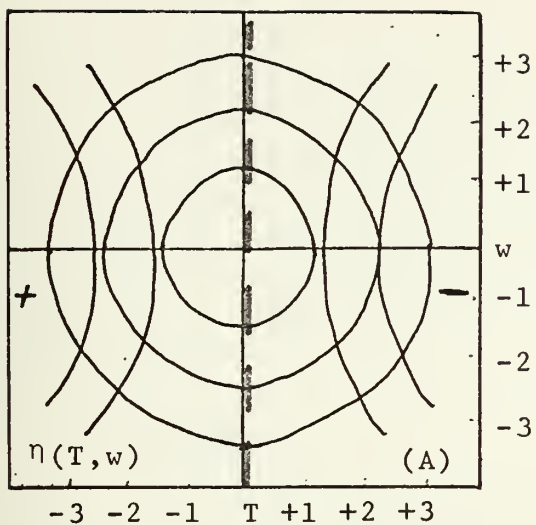


Figure 15. JDF/CMF results for period 1 subset 1.

1. Panel A

Temperature and vertical motion are shown as the JDF and wave height as CMF in this panel. When temperature is maximum positive and wave height is maximum negative. Likewise, the w maxima occur at every other inflection point of the wave.

2. Panel B

In this panel the CMF zero isolines separates the positive and negative phase of the temperature waveform. The JDF is the wave height and its derivative. The octants to be referred to were defined on page 30. This figure may be interpreted in a CCW direction starting in octant 1. Temperature may then be interpreted to show that when the wave height is negative the temperature is positive and vice versa. To state it another way, this panel represents a 180° phase shift between the ocean wave and temperature wave forms.

3. Panel C

The CMF zero isoline in this panel separates positive and negative vertical motion. The JDF is again determined from the wave height and its derivative. Interpretations of this panel in a CCW direction from octant 1 indicates that if the wave height is positive, w goes from positive to negative. This indicates a 90° phase shift between ocean waves and w wave forms during potential flow.

4. Panel D

The u and T are presented in the JDF and the CMF is for wave height. In octant 1 and 2 u and T are positive over the waves minima while in octant 5 and 6 u and T are negative over the wave maxima.

5. Panel E

Heat flux, wT , is the CMF and wave height and its derivative are the JDF in this panel. Beginning in octant 1, interpretation of this figure will describe heat flux in potential flow. During the positive phase of the wave wT completes a full negative and positive cycle with similar change for the negative phase of the wave. This indicates a 45° phase shift with respect to the wave.

6. Panel F

The CMF in this panel is u and the JDF is wave height and its derivative. Beginning in octant 1, interpretation of the panel shows that when the phase of the wave is positive the u waveform is negative and, therefore, a 180° phase shift. This is the same phase relationship shown for temperature in panel B. Attention will now be turned toward interpretation of results obtained from the four periods previously described.

C. PERIOD 1 RESULTS

Panels A and B of the JDF/CMF results, Figures 16, 17, 18 and 19, will be considered in detail for the following discussion. A cursory examination of the JDF/CMF patterns

in panel A and B of the above figures, in comparison to those in Figure 15 revealed that processes associated with potential flow are not the only ones that occurred. Specifically in Figure 16A there is a 135° - 315° orientation of the elliptical JDF pattern and the axis of the ellipse appears curvilinear. The elliptical pattern described above occurred in all remaining subsets of this period, Figure 17A, 18A and 19A, and during all periods considered in this study. This indicates approximately a 180° phase shift in w and T instead of the 90° observed in Figure 15 when potential flow was considered. The 90° CCW rotation of the CMF wave height pattern indicates that in general a w minima and T maxima occur over the wave crest.

The latter phase relationships are also apparent in the phase amplitude results in Figure 20. For potential flow temperature maxima occurred over the wave trough and w was 90° out of phase with respect to the wave. A number of smaller perturbations appeared in the T waveform of Figure 20. They could be due to the turbulent contribution suggested by Volkov (1969).

A possible physical interpretation of the phase relationship noted above could be that at a fixed observation level the waves are causing a transfer of warmer air downward and colder air upward thereby inducing a net heat transfer downward. This was not apparent, however, in the spectral results, Figure 12, 13 and 14, where it was observed that significant spectral peaks do not appear in T or wT at a

predominate frequency of the wave spectrum. Temperature and w JDF and η CMF relationships throughout the remainder of Period 1 appear in panel A of Figures 17, 18 and 19. The CMF patterns in panel A of the above figures are no longer rotated 90° CCW from potential flow but are approximately 45° . The 45° rotation is most evident in the large wave class region, greater than 1.5σ , of the JDF array. Figure 18A is an excellent example of this change in rotation. An evaluation of the JDF/CMF results of Figure 18 in conjunction with phase amplitude results in Figure 22 reveals that w and T are approximately 45° out of phase. Potential flow results had indicated a 90° phase shift. The temperature maxima, considering only the larger crests, are almost in phase with the wave trough which indicates a tendency toward potential flow.

Changes in thermal stratification throughout the period may have been a factor in these results. The thermal stratification changed from near neutral to stable and returned to near neutral during the course of the period. The Z/L values changed from -0.03 to -0.20 and ended at -0.08 . Therefore, with respect to stability and the above results one can say that under greater stability there was a tendency toward potential flow as shown in Figure 18A and 22, and there were fewer perturbations on the basically sinusoidal temperature waveform as shown in Figure 22. Furthermore, it was observed in Figure 19A and 23 that as thermal stratification returned

toward neutral the JDF/CMF results deviate more from potential flow conditions than was observed in Figure 18A and 22 discussed above.

Another feature apparent in panel A of Figures 16, 17 and 18 is that the large wave class results near the outside of the array return to potential flow predictions more so than the small wave class results.

Panel B of Figures 16, 17, 18 and 19 provided information on the phase relation of temperature with respect to the wave. Corresponding phase amplitude summaries for these JDF/CMF arrays appear in Figures 20, 21, 22 and 23. JDF/CMF results in Panel B appear to be more sensitive to changes in thermal stratification than those in panel A. For example, an examination of Figure 16B reveals positive temperature over the wave crests while a similar comparison of Figure 17B reveals negative temperature over the wave troughs. Similarly an examination of Figure 18B reveals negative temperature over the wave crests as the period becomes more stable. In general the JDF/CMF and phase amplitude patterns became less well defined as the period progressed and thermal stratification became more neutral. As an example, compare Figure 18B with 19B.

Again the small wave class results differ more from potential flow prediction than the large wave class results.

Vertical action in association with the ocean waves also appears in panel C of Figures 16, 17, 18 and 19. This series of panels cannot be readily interpreted for phase relations

between the w waveform and the ocean waves. Summarized phase amplitude results for w and the waves appear in Figures 20, 21, 22 and 23. The results of these figures also show that there is a w maxima ahead of the wave crest. For the potential flow case, there would be a 90° lead.

JDF results for the joint occurrence of u and T with respect to the CMF of the wave height appear in panel D of Figures 16, 17, 18 and 19. The 045° - 215° orientation of the JDF ellipse indicates u and T are positively correlated as predicted by potential flow. However, the curvilinear shape of the axis of the ellipse represents a deviation from potential flow theory. The CMF zero isoline for wave height in panel D is rotated 45° CW from the potential flow orientation. This indicates a phase shift of both u and T with respect to the wave. Summarized phase amplitude results for u and T appear in Figures 20, 21, 22 and 23.

D. PERIOD 2 RESULTS

Thermal stratification was slightly stable at the beginning of the period and became near neutral as the period progressed as indicated by Z/L values changing from -0.00 to -0.01. Only the first two subsets of the form will be discussed for this period because all subsets, in contrast to those just described for period 1, are quite similar. Subset 3 and 4 results appear in Appendix A in Figures 32, 33, 34 and 35.

In general results reveal deviations from potential low conditions. This can be readily noted by comparing patterns

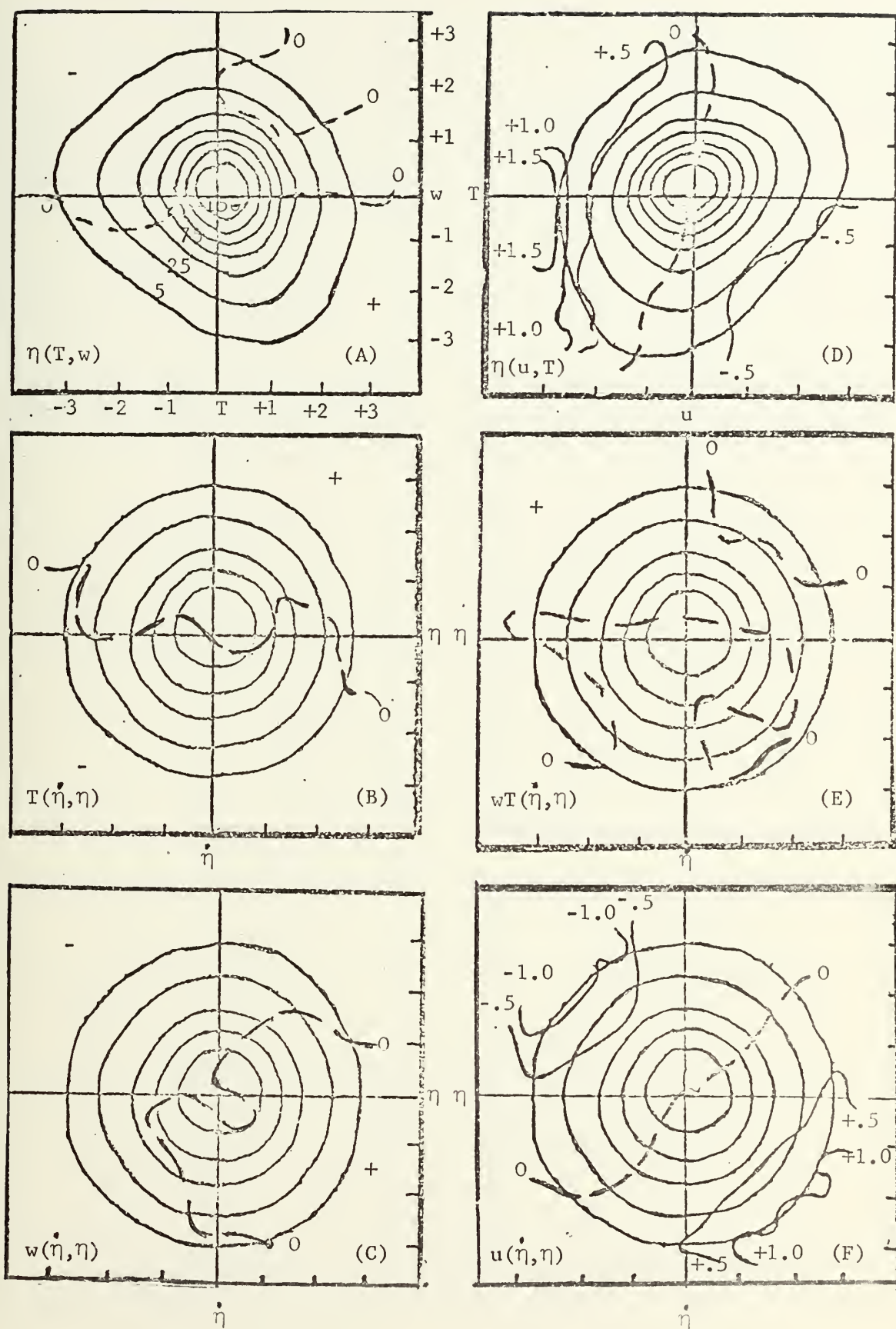


Figure 16. JDF/CMF Results for period 1 subset 1.

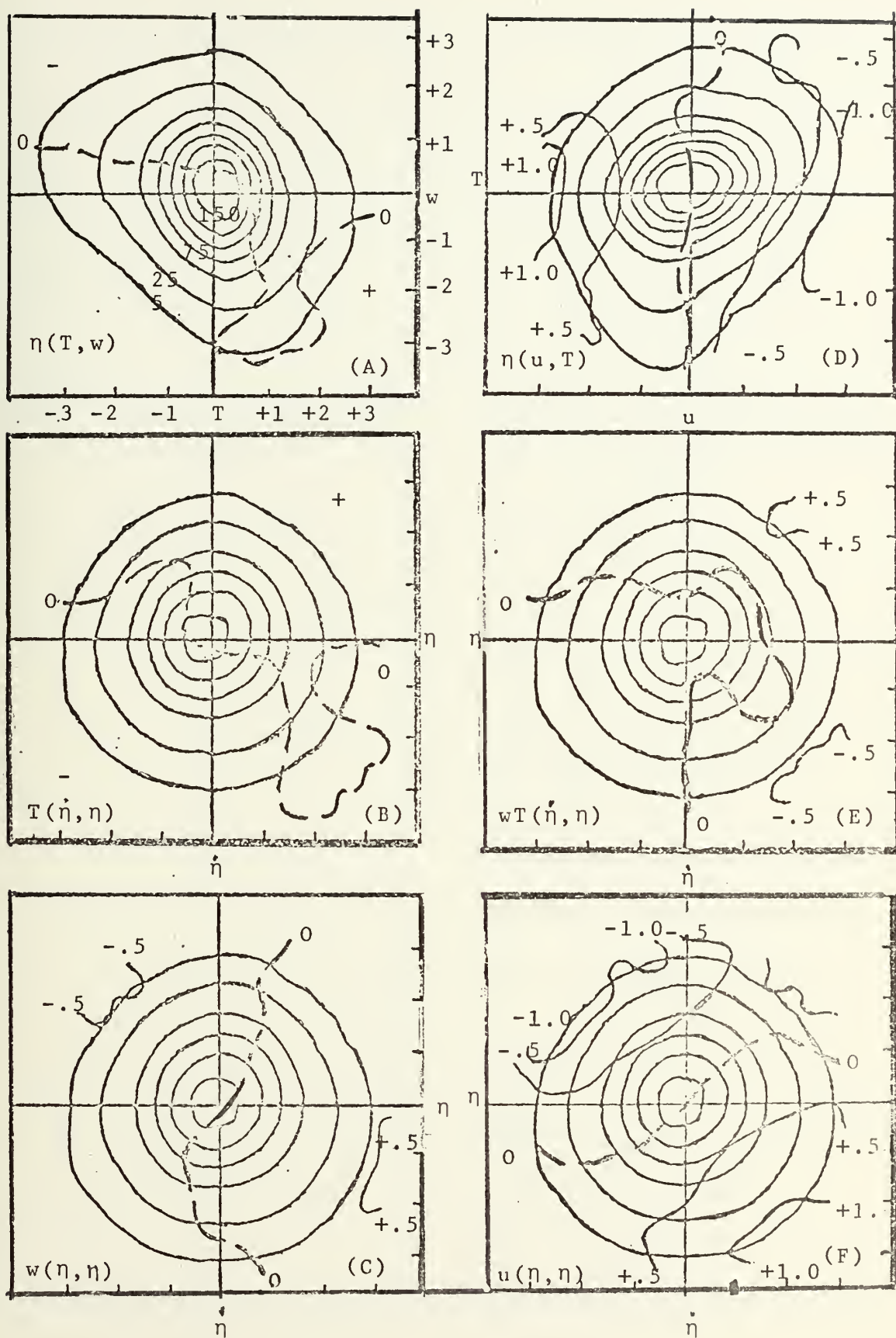


Figure 17. JDF/CMF Results for period 1 subset 2.

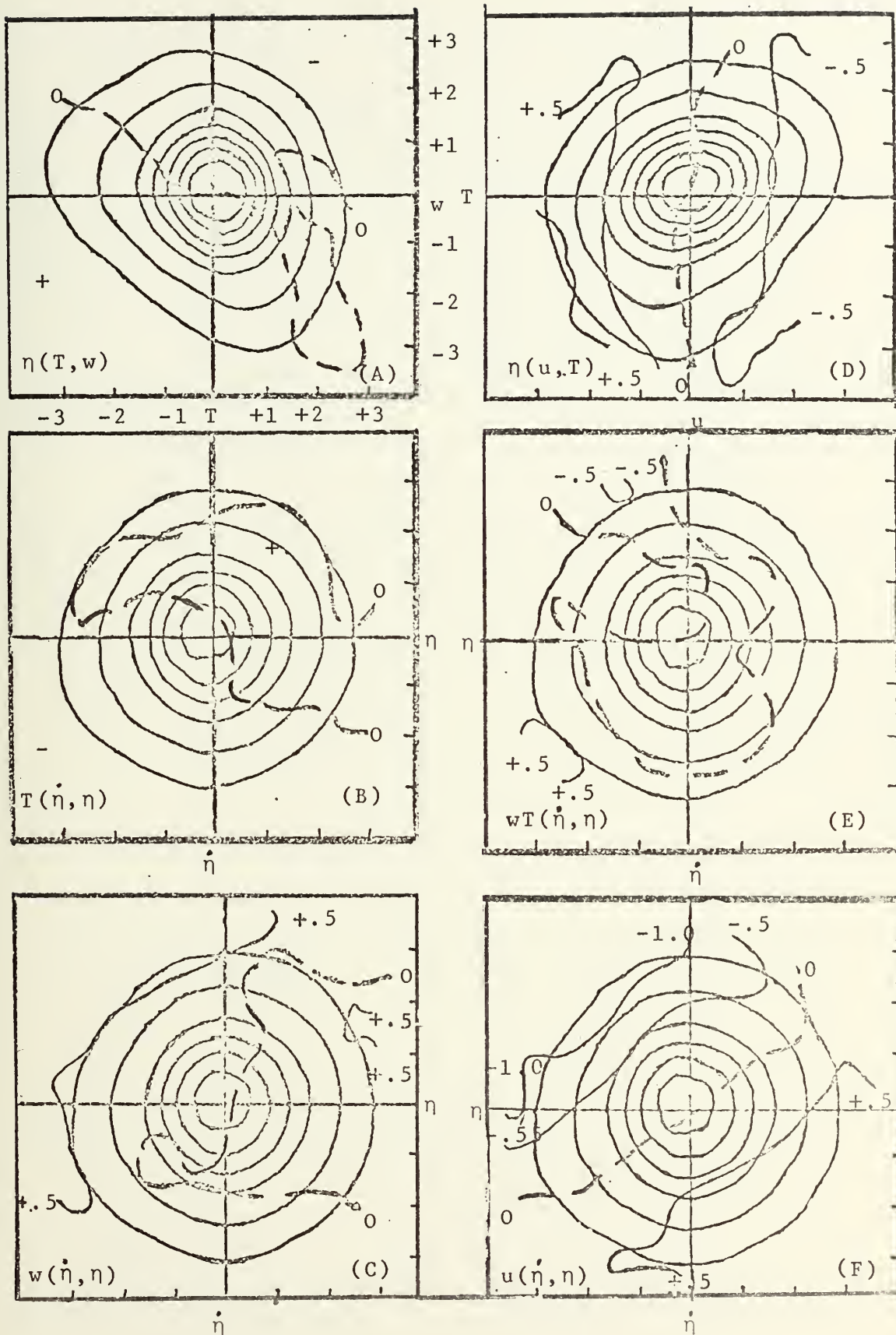


Figure 18. JDF/CMF Results for period 1 subset 3.

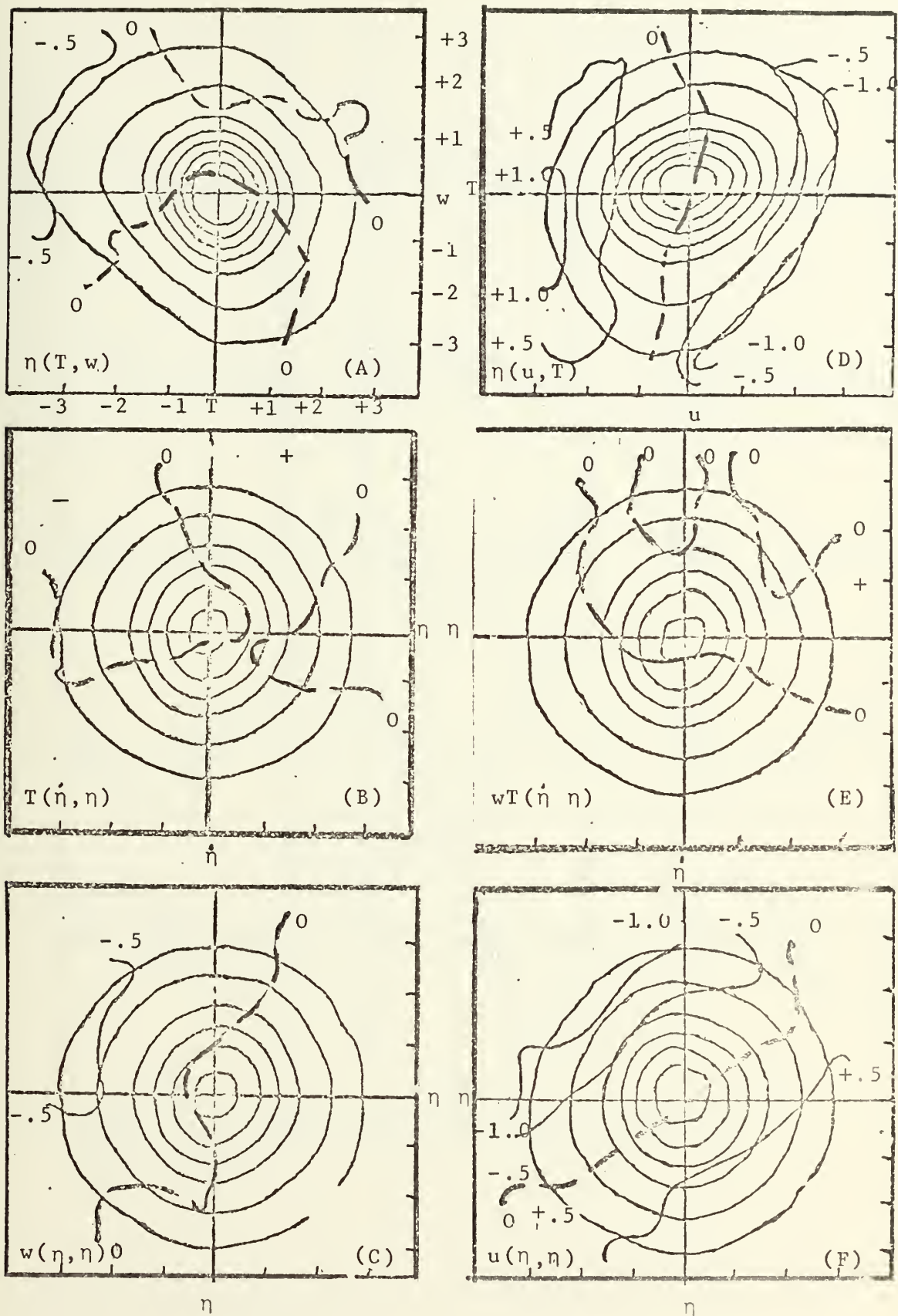


Figure 19. JDF/CMF Results for period 1 subset 4.

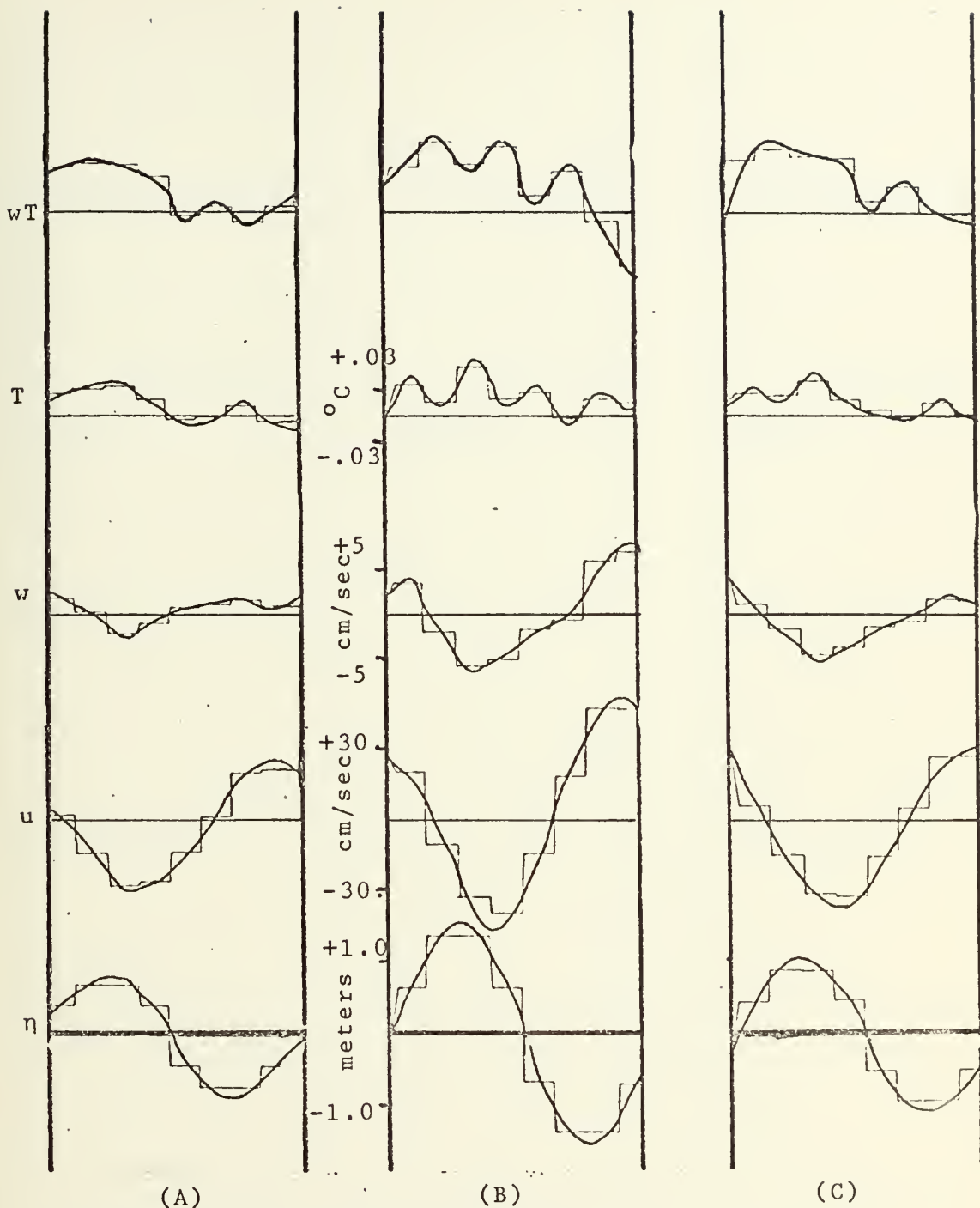


Figure 20. Phase amplitude results for period 1 subset 1 (a) small waves, (b) large waves, and (c) all waves.

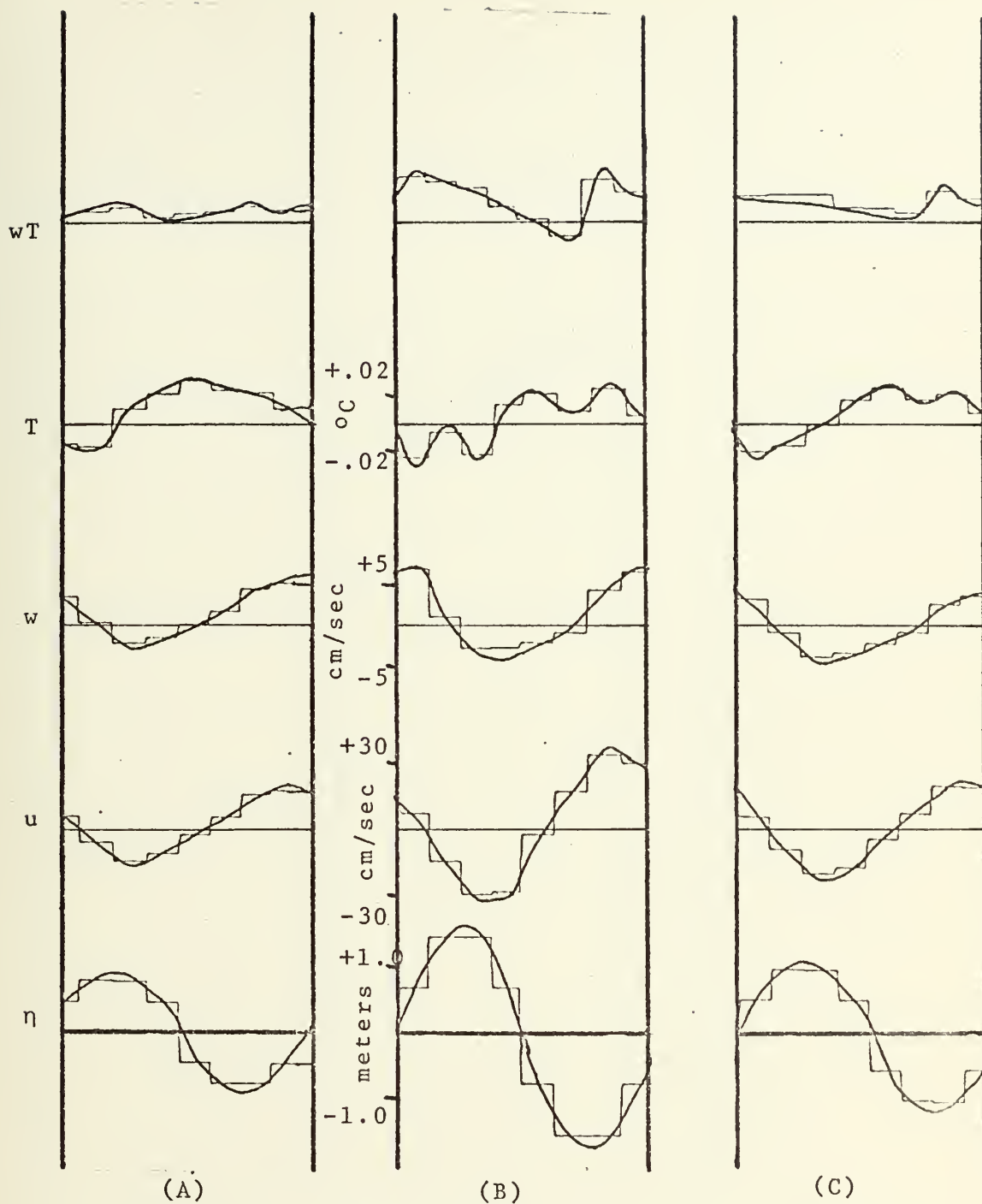


Figure 21. Phase amplitude results for period 1 subset 2 (a) small waves, (b) large waves, and (c) all waves.

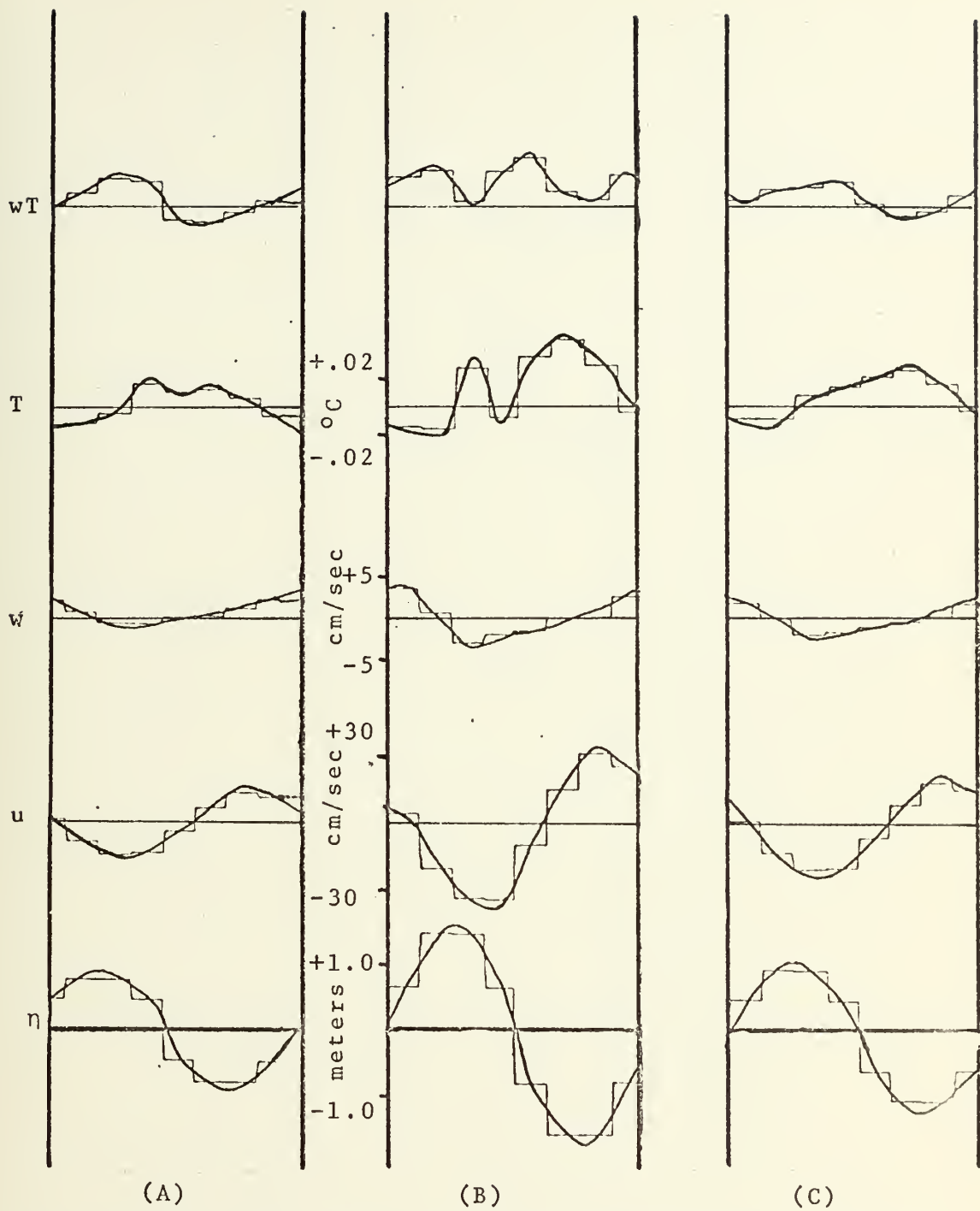


Figure 22. Phase amplitude results for period 1 subset 3 (a) small waves, (b) large waves, and (c) all waves.

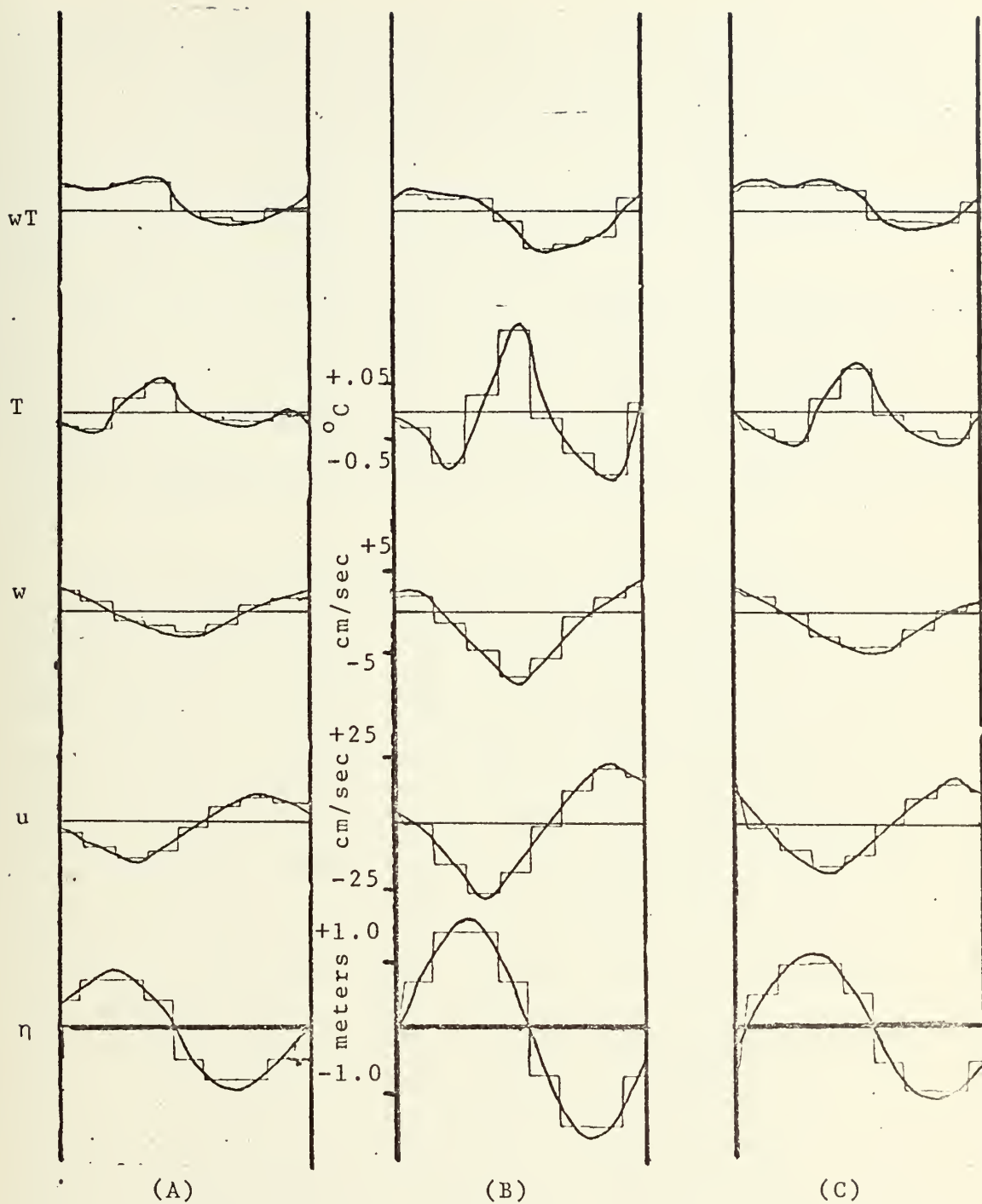


Figure 23. Phase amplitude results for period 1 subset 4
 (a) small waves, (b) large waves, and (c) all waves.

in Figures 24 and 25 with results in Figure 15. Specifically, the CMF zero isoline in Figure 24A has a 45° CCW rotation from potential flow orientation, Figure 15A. A similar rotation was observed in Figure 18A which corresponds to the more stable conditions in Period 1.

The T and w/JDF results are elliptical in Figure 24A as in Period 1 and has a 315° - 135° orientation. This again suggests a 180° phase shift between T and w in contrast to the 90° predicted by potential flow theory shown in Figure 15.

Relationships between features in this period and the thermal stratification can be further examined by a broad comparison of similar JDF/CMF panels in Figure 24 and 25. The patterns in Figure 24 appear to have fewer small scale perturbations than those in Figure 25. Phase results for this period are summarized in the phase amplitude results in Figures 26 and 27. It can be noted that the results in Figure 27 in contrast to the JDF/CMF results in Figures 25 are more readily examined even though small scale perturbations occur. An example is the temperature waveform in Figure 27. Thermal stratification was near neutral during the second subset corresponding to Figure 27. This deviation from a sinusoidal waveform, as for Period 1, is considered to be due to turbulence.

With respect to different wave classes, small wave classes appear to approach potential flow features more than the larger wave classes. This feature is shown by the ve

height CMF zero isoline in Figure 24A. This is in contrast to their tendency to deviate from potential flow as was observed in Period 1 during more thermally stable conditions.

A feature that did not appear in Period 1 but appears in this period is the tendency for the temperature waveform to have sharper crests and troughs than the ocean waves.

E. PERIOD 3 RESULTS

Hydrostatic conditions throughout this period were stable with a Z/L value of approximately -0.12 . Results for this period were quite similar to those presented for subsets 2 and 3 of period 1, Figures 17 and 18. The latter subsets also occurred during more stable conditions.

Since all three subsets of this period were similar, only subset 1 will be discussed in detail. Results for subsets 2 and 3 are in Appendix A as Figures 36, 37, 38 and 39.

The JDF of u and T and the CMF of wave height appear in Figure 28A. The CMF zero isoline in Figure 28A is rotated approximately 70° CCW from potential flow results, Figure 15. Phase amplitude results in Figure 29 indicate the above rotation is due to the temperature waveform being shifted approximately 45° from the wave's trough. This is to be expected in view of previous results when thermal stability, in terms of Z/L values, was considered. During period 1, Z/L values varied from -0.03 to -0.20 to -0.08 and maxima in the temperature phase amplitude varied from 180° out of phase with the wave trough, Figure 23, to approximately in phase

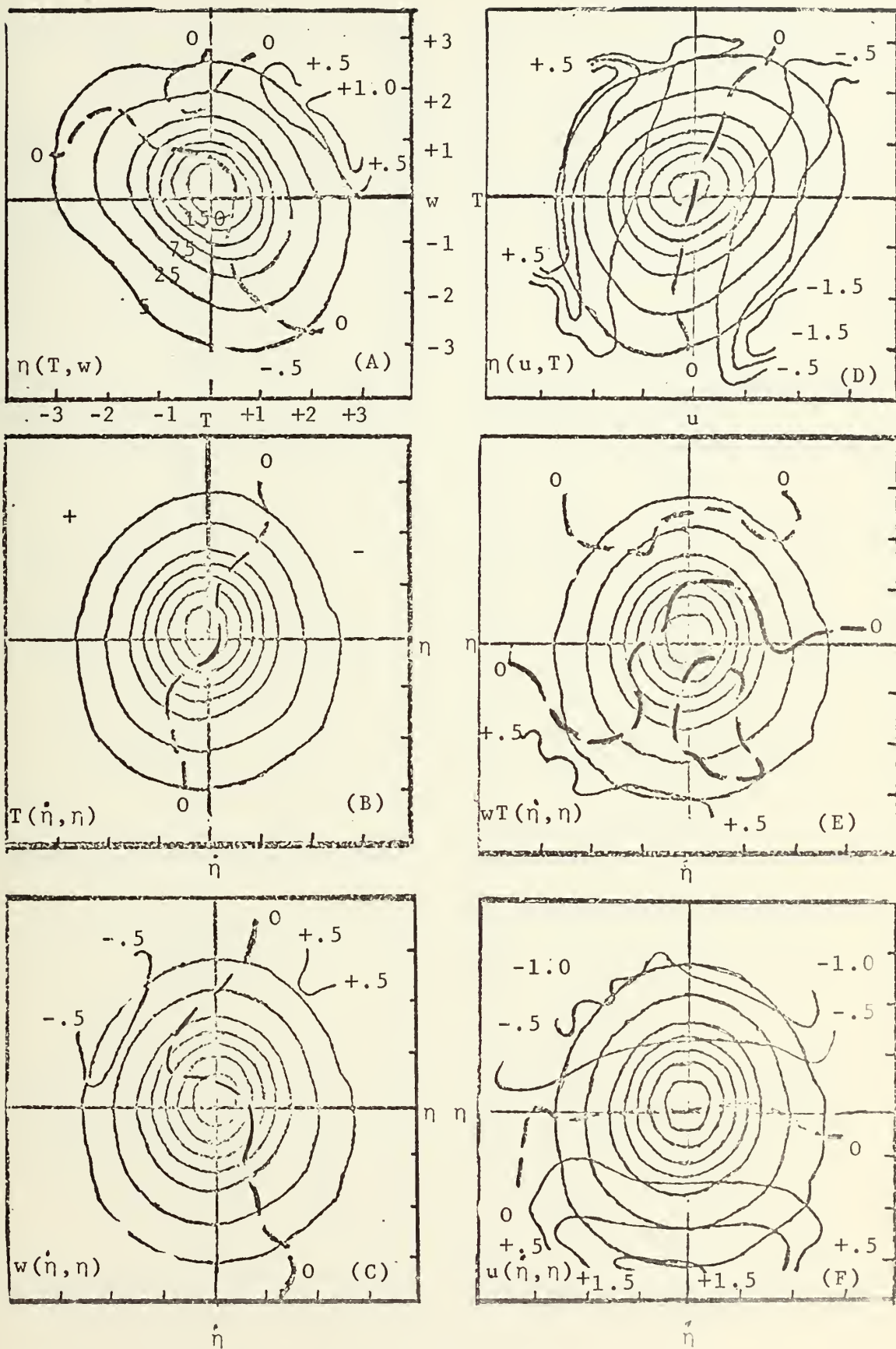


Figure 24. JDF/CMF Results for period 2 subset 1.

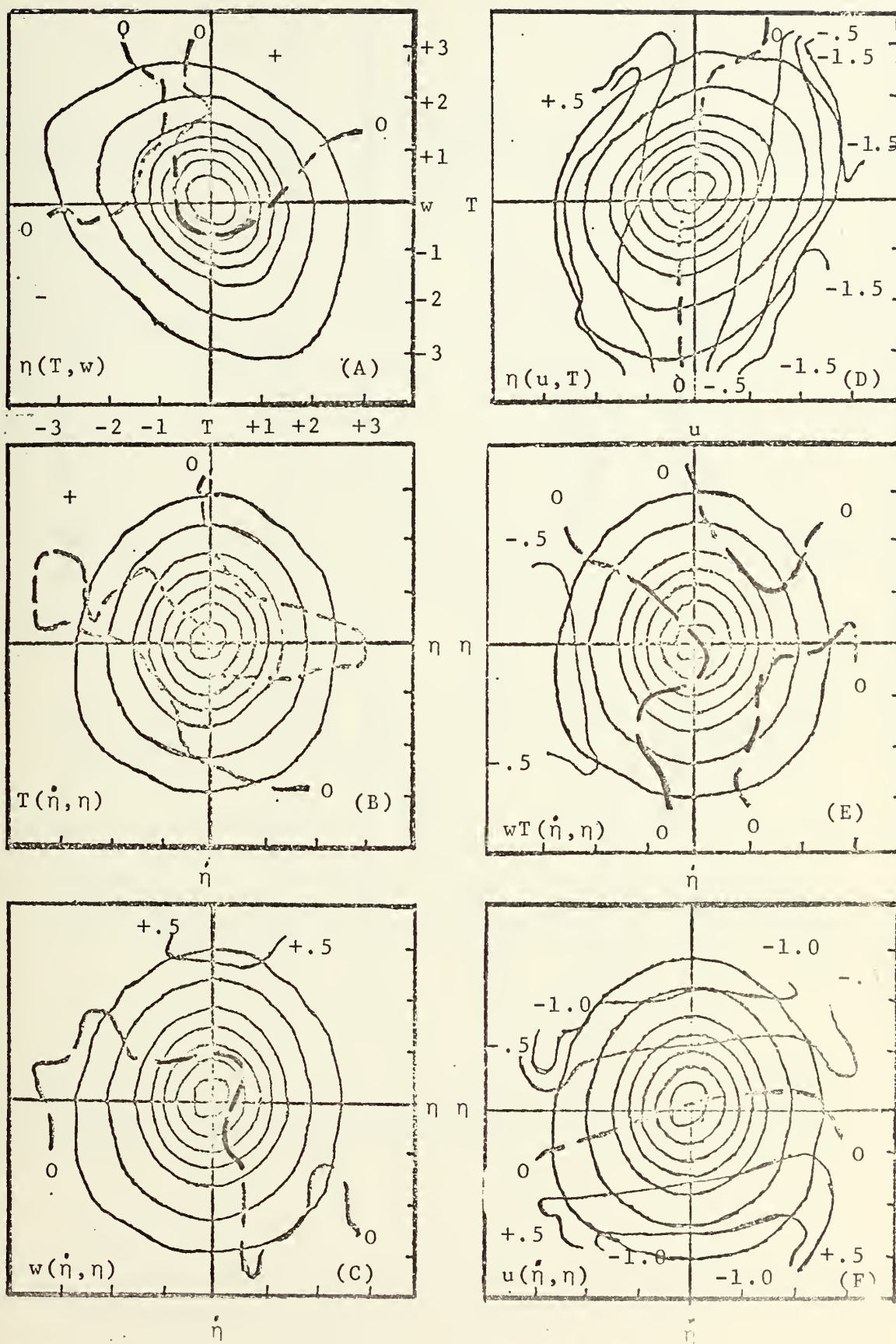


Figure 25. JDF/CMF Results for period 2 subset 2.

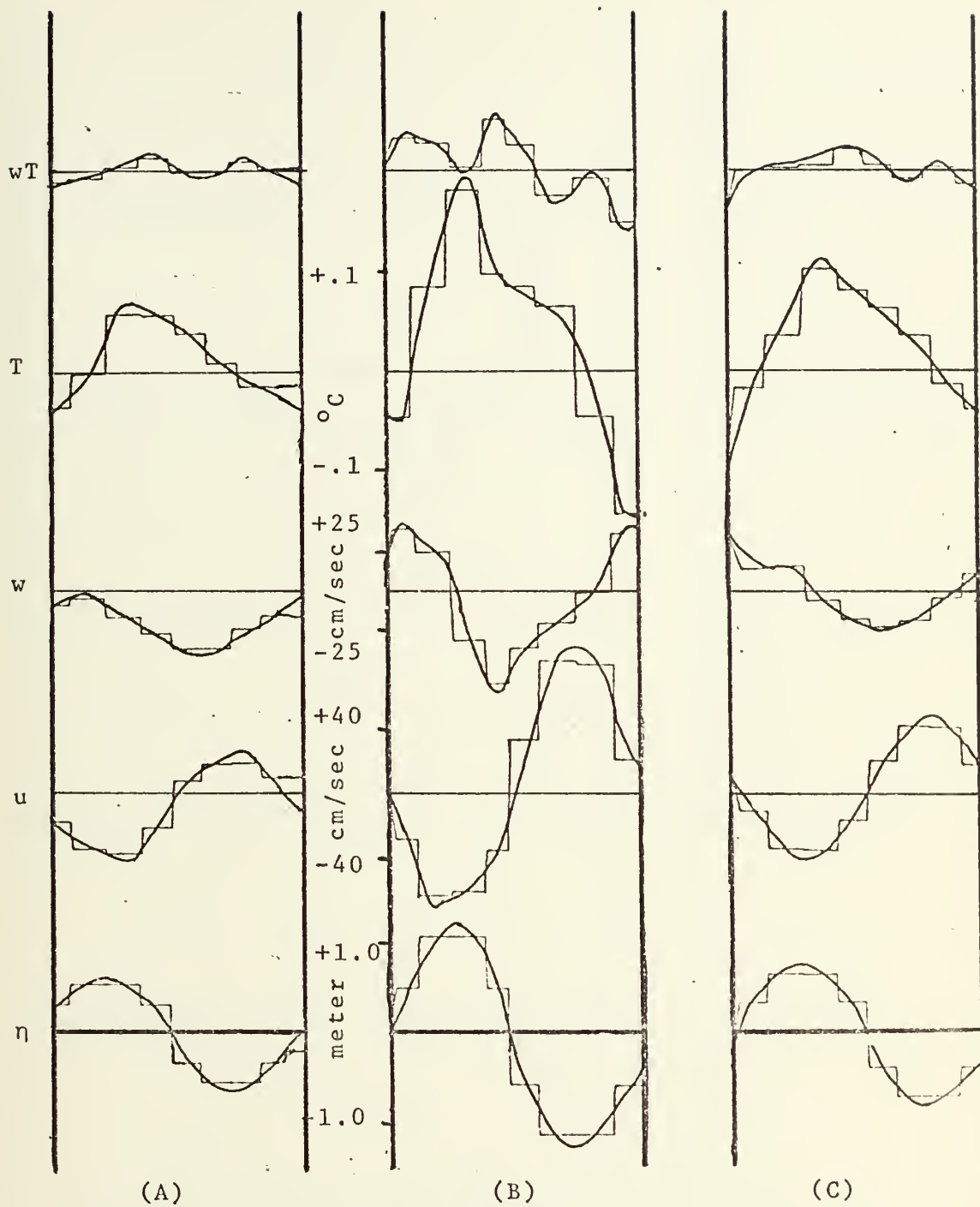


Figure 26. Phase amplitude results for period 2 subset 1 (a) small waves, (b) large waves, and (c) all waves.

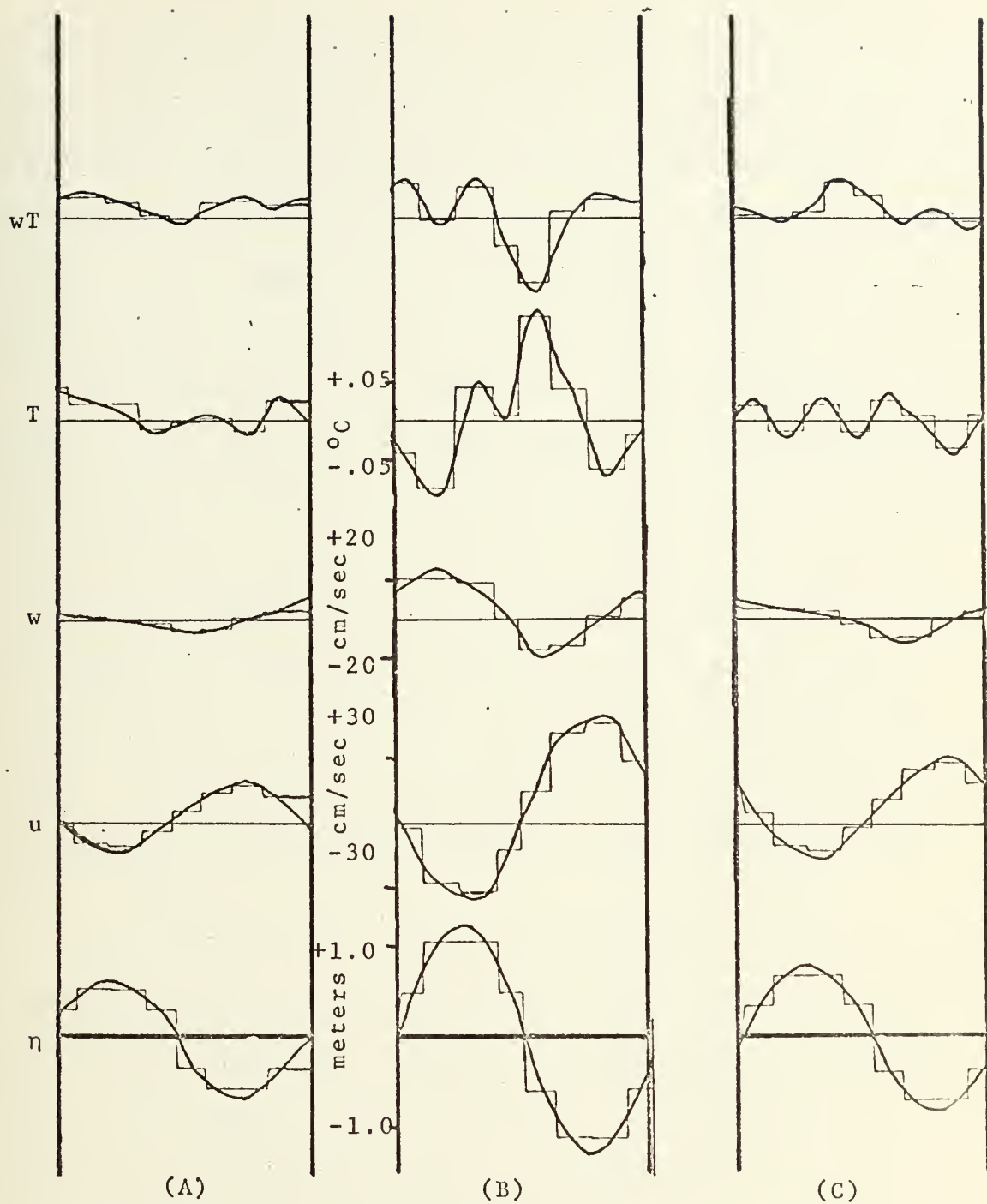


Figure 27. Phase amplitude results for period 2 subset 2 (a) small waves, (b) large waves, and (c) all waves.

with the wave trough, Figure 20. Period 3, however, has a consistent Z/L value of about -0.12 . Therefore, phase differences between temperature and waves during period 3 were between the extremes noted in period 1. This can be readily observed by a comparison of the phase amplitude results for T and waves in Figure 20 and 23 to those in Figure 29.

With respect to wave amplitude classes, small and large waves appear to have the same deviation from potential flow. This is most evident by a comparison of the wave height CMF zero isoline in Figure 28A and in Figure 15. Recall that during the changing stability associated with period 1, only the small wave amplitude classes had a tendency toward potential flow, Figure 18A. This is in contrast to the results during the near neutral conditions during period 2 where small waves had a tendency toward potential flow, Figure 24A.

Panel 28B and 28C results show the CMF variables T and w respectively compared to the JDF of the wave height and its derivative. CMF zero isolines in both panels are shifted away from potential flow, Figure 15. In addition, panels 28B and C display fewer small perturbation than similar results obtained in period 1, Panel B or C of Figures 16, 17, 18 and 19 or period 2, Panel B and C of Figures 24 and 25. This again was probably associated with the turbulence occurring during the period.

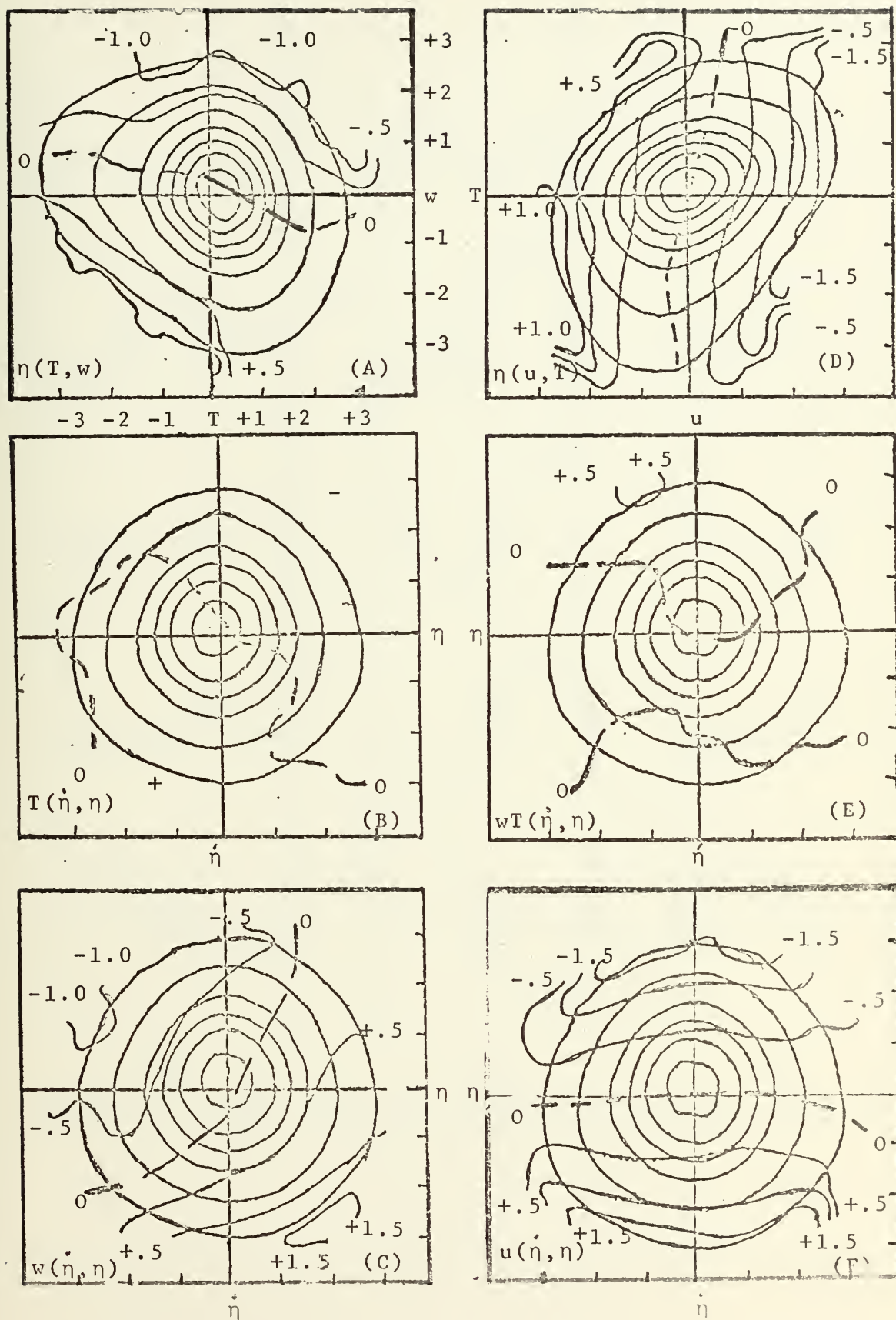


Figure 28. JDF/CMF Results for period 3 subset 1 (a) small waves, (b) large waves, and (c) all waves.

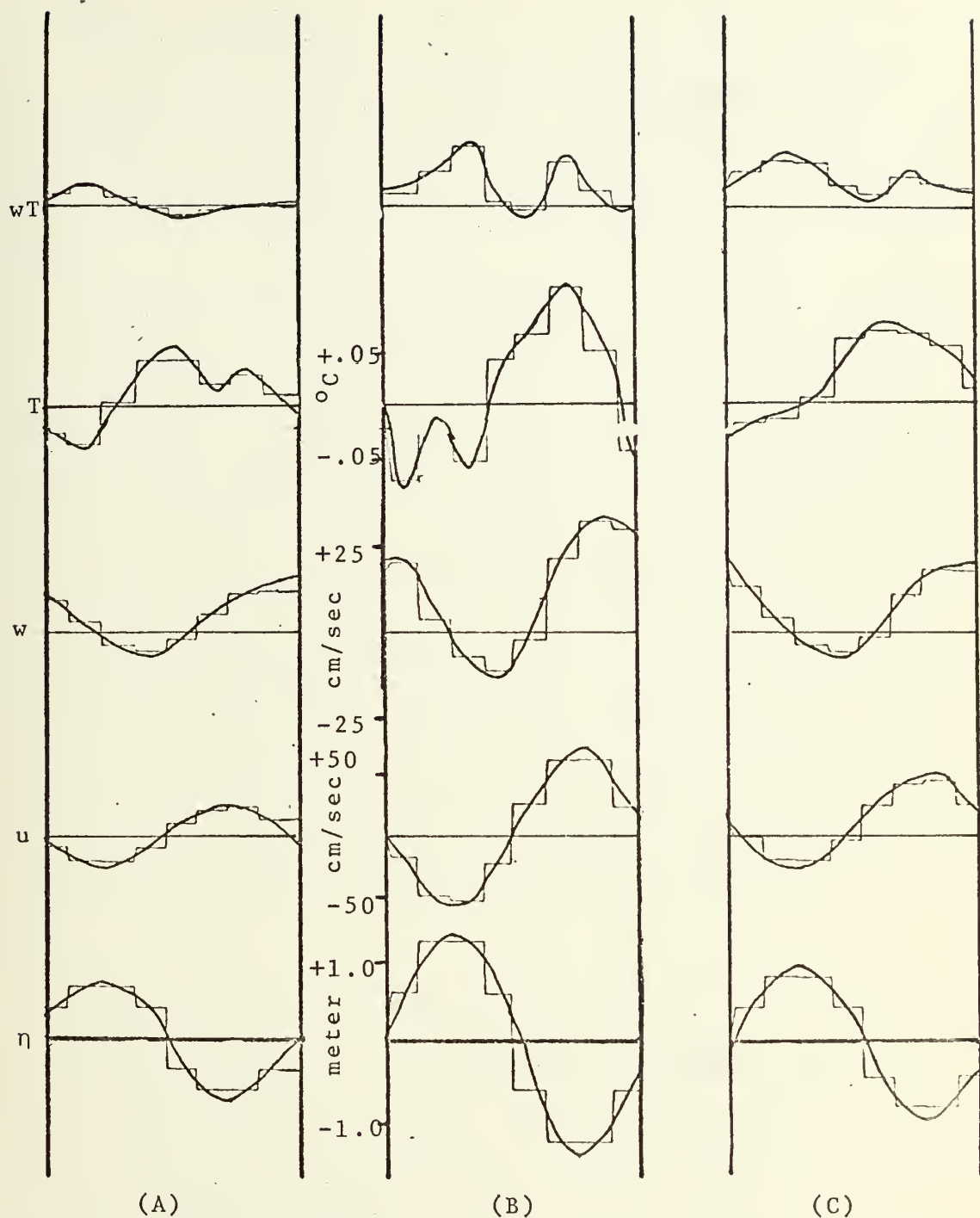


Figure 29. Phase amplitude results for period 3 subset 1 (a) small waves, (b) large waves, and (c) all waves.

F. PERIOD 4 RESULTS

Results are similar to those in Period 3. The value of the thermal stability parameter, Z/L , averaged -0.12 in this period but approaches neutral conditions near the end of the period.

The period ended with a Z/L value of -0.05 . Even though the stability decreased during period 4 the results were quite similar to those obtained for period 3. However, the near neutral conditions did not occur until the very end of the period and, thereby, suggest that some time lag occurred after the long interval of stability in period 3 before the wind wave coupling adjusted to the new environment and the analytical method used could detect changes. Due to the similarity of results for this period, only the first of the 3 subsets will be used for discussion. Results for the last two subsets are presented in Appendix A, Figure 40, 41, 42 and 43.

Results for this period, shown in Figure 30, are similar to those for period 3. For example, in Figure 30A, the temperature maxima is 45° from the wave's trough as was the case during period 3, Figure 28A. Phase amplitude results are shown in Figure 31.

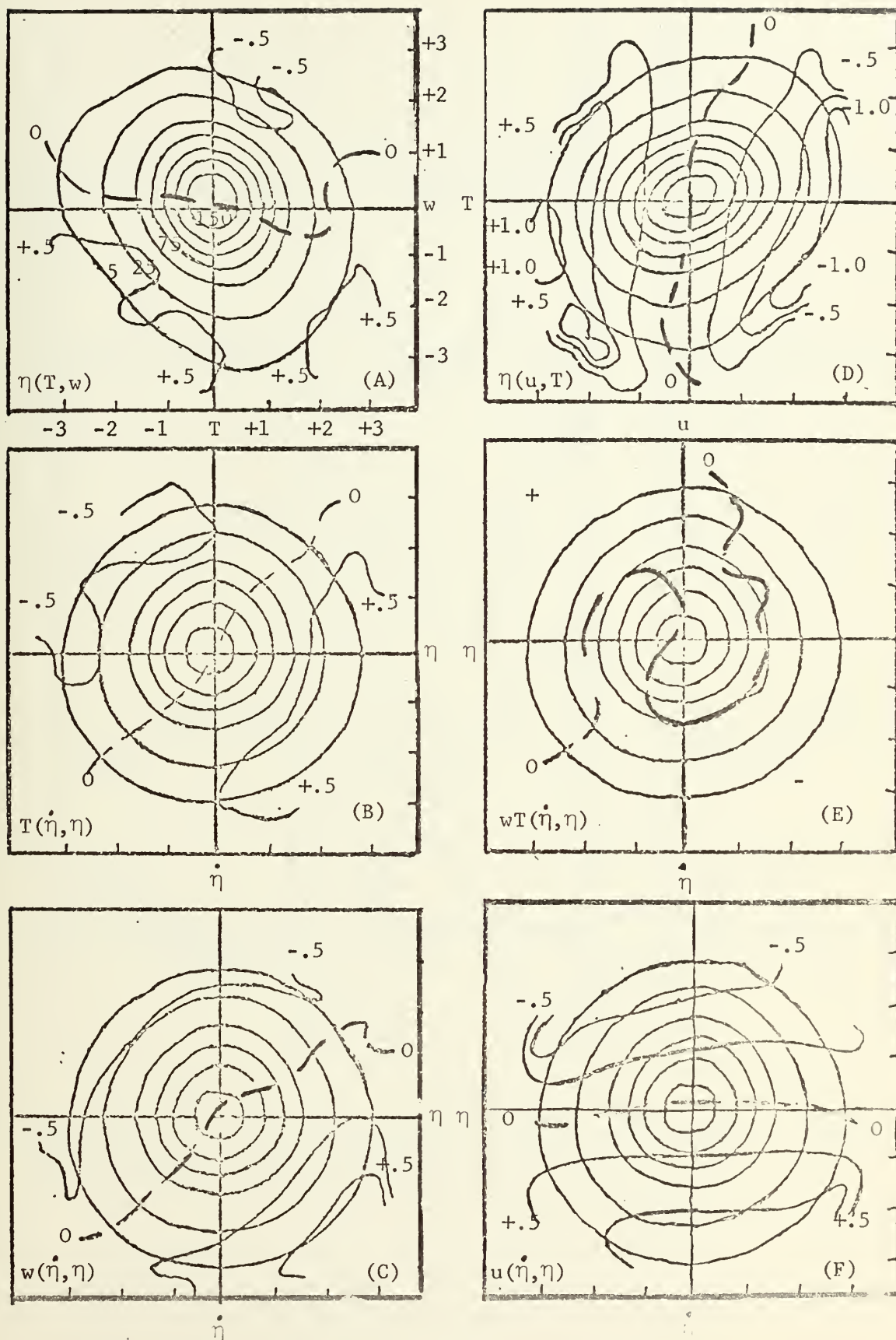


Figure 30. JDF/CMF Results for period 4 subset 1.

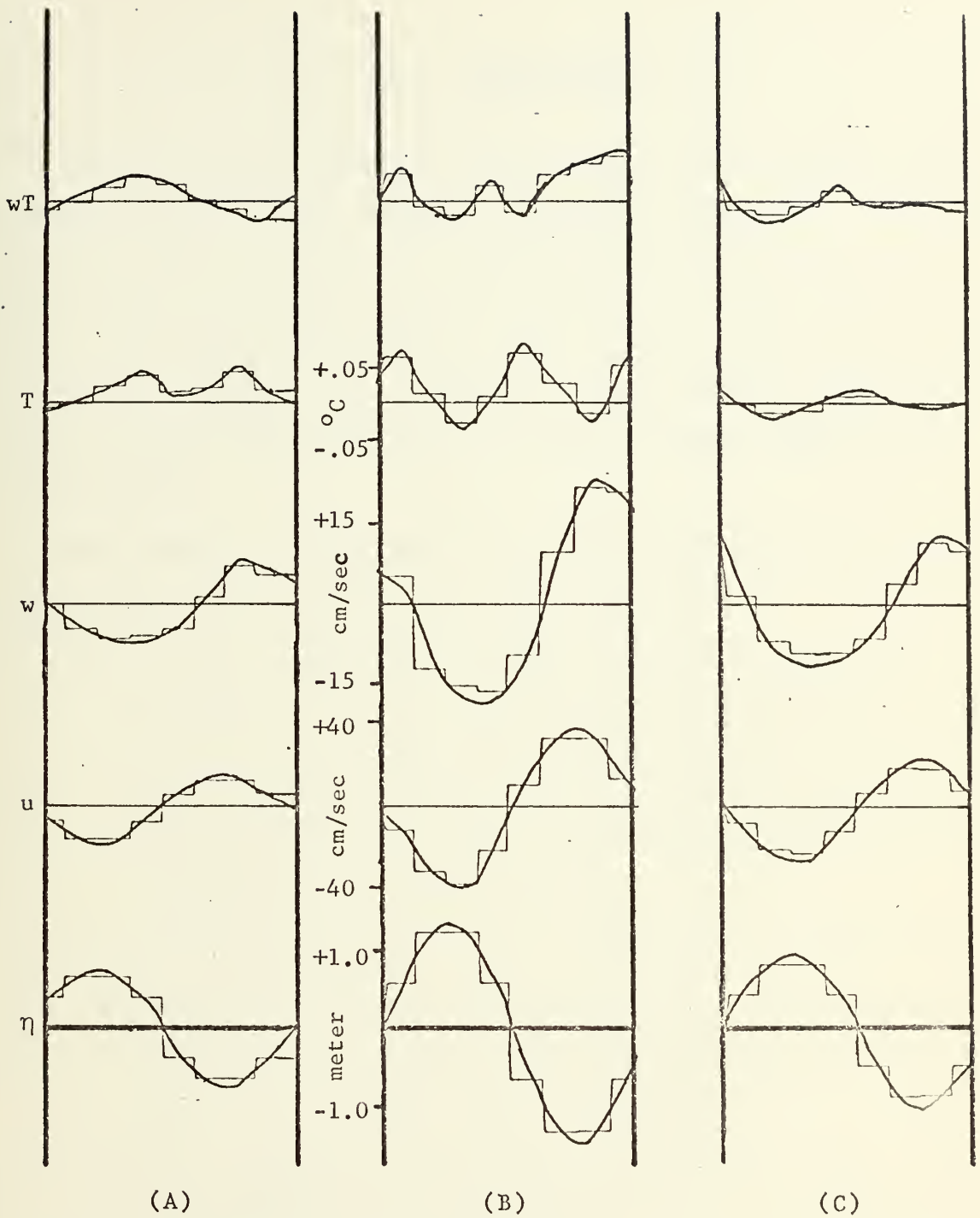


Figure 31. Phase amplitude results for period 4 subset 1 (a) small waves, (b) large waves, and (c) all waves.

VII. CONCLUSIONS

This study has been an investigation of turbulence data obtained during near neutral to stable conditions. The temperature fluctuations, were described with respect to the wave's influence over natural ocean waves. The statistical procedure, JDF/CMF, was used which made possible interpretation of nonlinear properties of wave induced temperature fluctuation.

The general characteristic of observed temperature wave-forms leads to the following conclusions.

1. The most important property shown is that waves influence a scalar field such as temperature as high as 8 meters. Therefore, observational studies conducted over ocean waves must consider the wave's influence on a scalar field.
2. The suggestion by Volkov (1969) that a temperature observation at a fixed level above a wave surface is composed of a mean, a fairly well organized fluctuation due to waves, and a fluctuation due to turbulence appears to be valid. All periods show small fluctuations superimposed on a more uniform sinusoidal wave induced fluctuation.
3. The phase shift of temperature away from wave crests is $0-135^{\circ}$ with an average about 84° for all periods. This is in contrast to the 180° phase shift predicted by potential flow.

4. The temperature profile leads the vertical velocity although it may have a maximum of 45° on either side of the wave crest. This is in contrast to the 90° shift predicted by potential flow.
5. As stated in the background, Stewart (1969) did not consider waves capable of influencing a scalar temperature field. Therefore, he considered vertical velocity and T phase angles near zero or 180° indicative of mostly turbulence and angles $\pm 90^{\circ}$ indicative of waves. This study has shown that under stable conditions neither extreme is attained. The reason for not consistently being at either extreme is possibly due to the wave induced fluctuation.
6. It also appears for this one study that if the atmosphere is neutral or very stable for an extended period, sea-air coupling will tend toward, but probably never reach, potential flow characteristic. In between these two extremes, the greatest deviation from potential flow will be seen.

This study shows that JDF/CMF statistical technique is very promising and should be applied to other data obtained during the same period. Such a study would determine if the conclusions of this study are consistent. Unstable periods should be included if available.

One possible application presented for this type of study was its use in predicting laser propagation. With more studies of this type it should become possible to

predict the temperature fluctuations under different thermal stratifications. Therefore, with a knowledge of the thermal stratification and the wave field below, a more accurate refractive index corrected for the wave's influence could be provided to laser users.

APPENDIX A

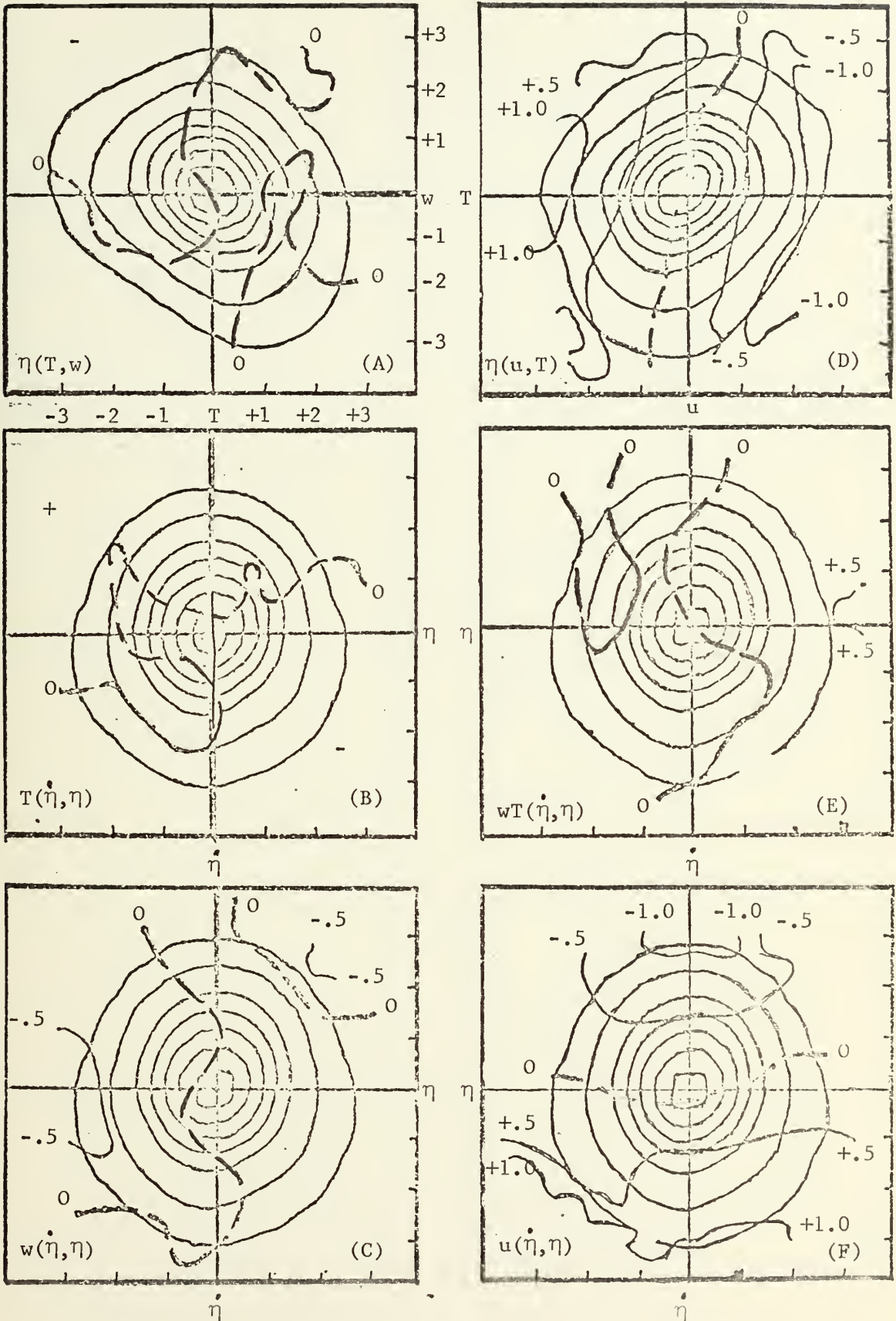


Figure 32. JDF/CMF Results for period 2 subset 3.

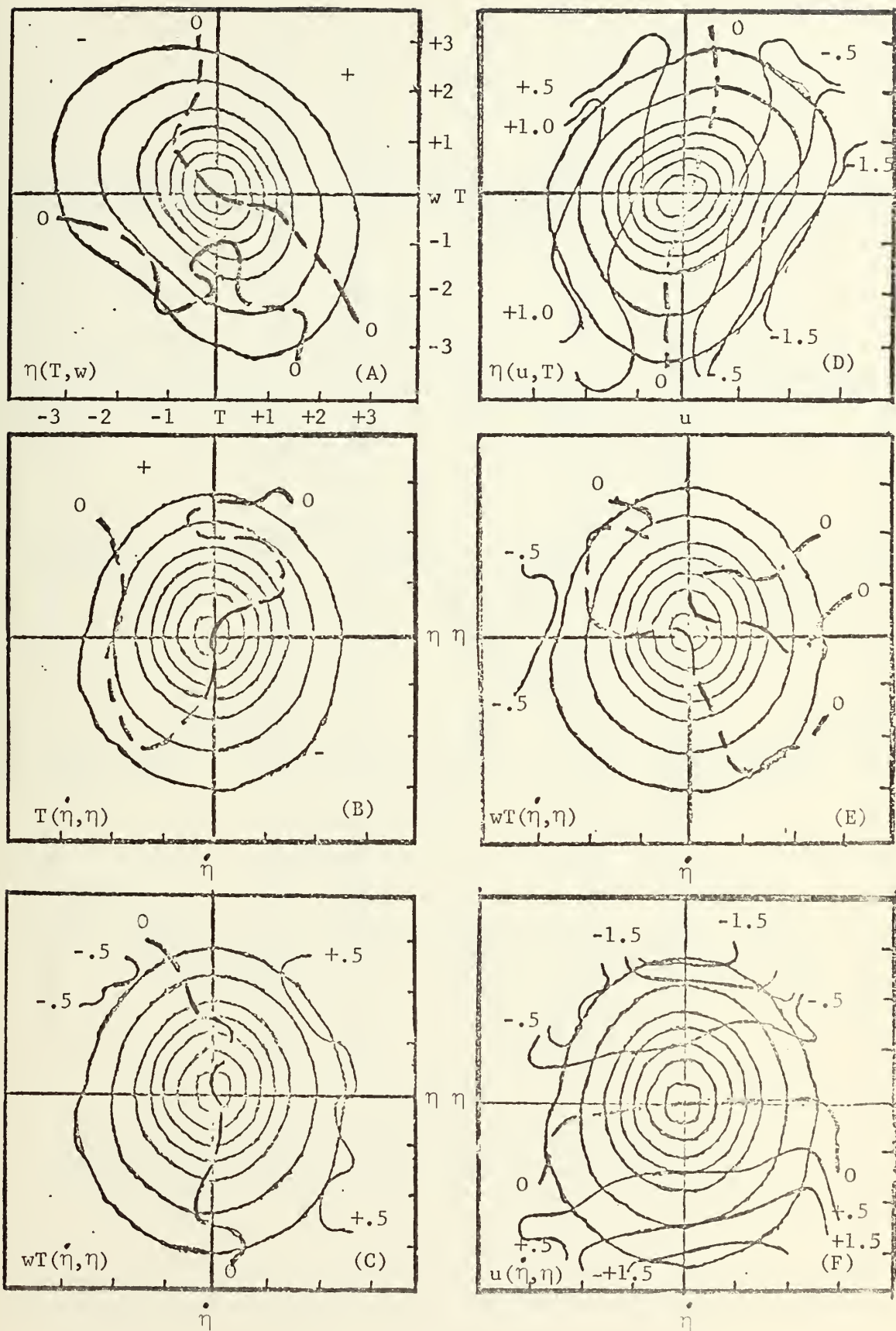


Figure 33. JDF/CMF Results for period 2 subset 4.

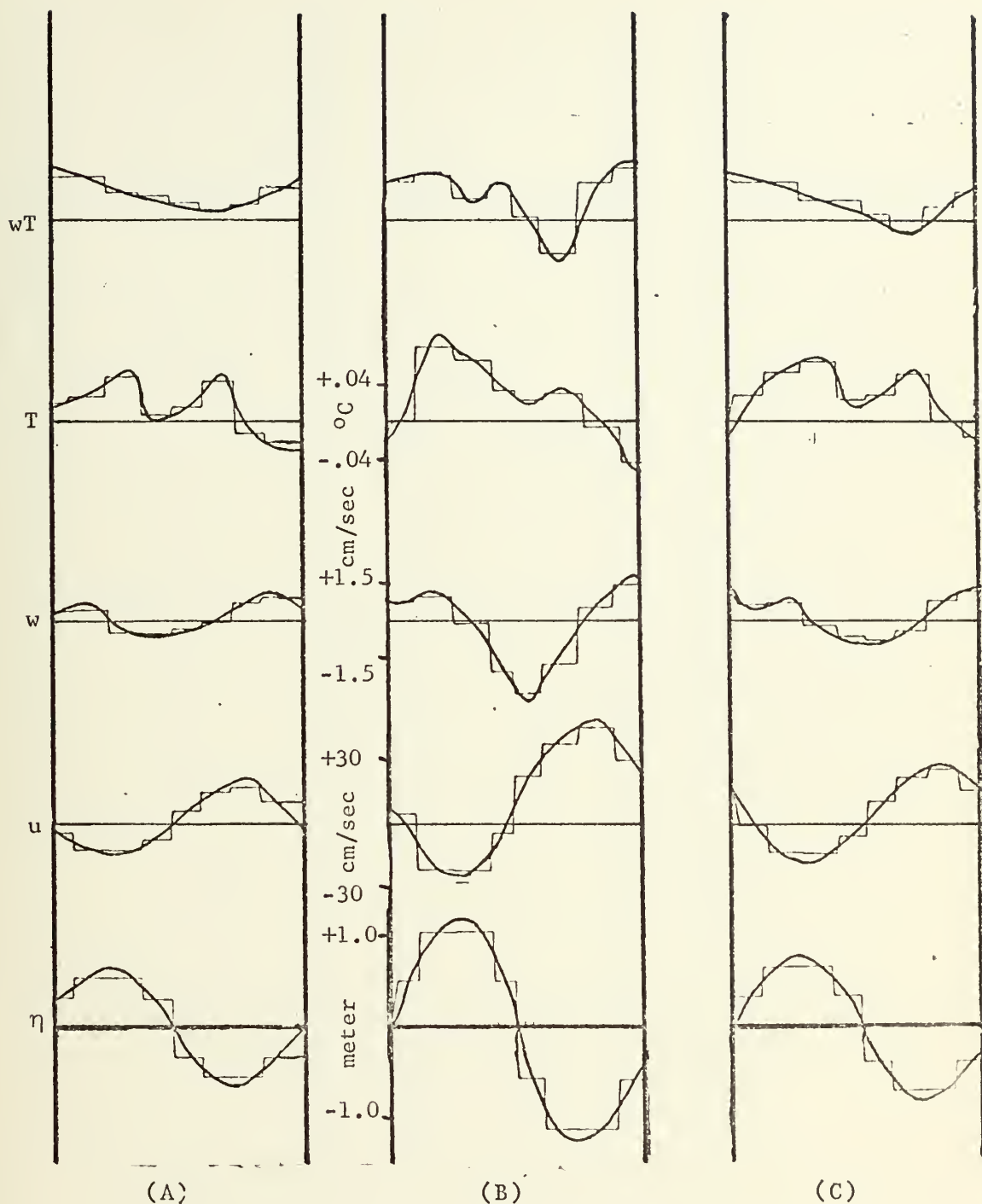


Figure 34. Phase amplitude results for period 2 subset 3 (a) small waves, (b) large waves, and (c) all waves.

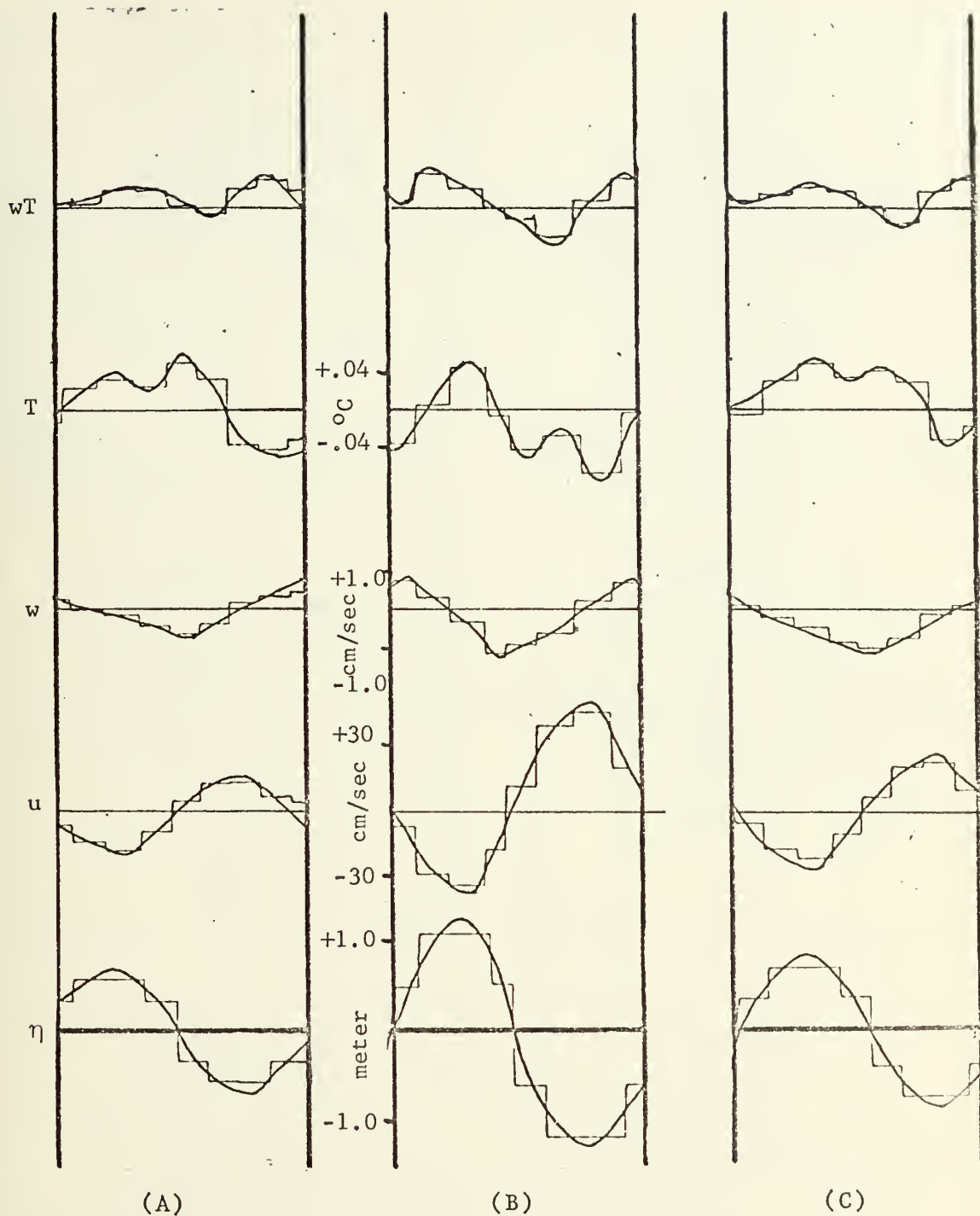


Figure 35. Phase amplitude results for period 2 subset 4 (a) small waves, (b) large waves, and (c) all waves.

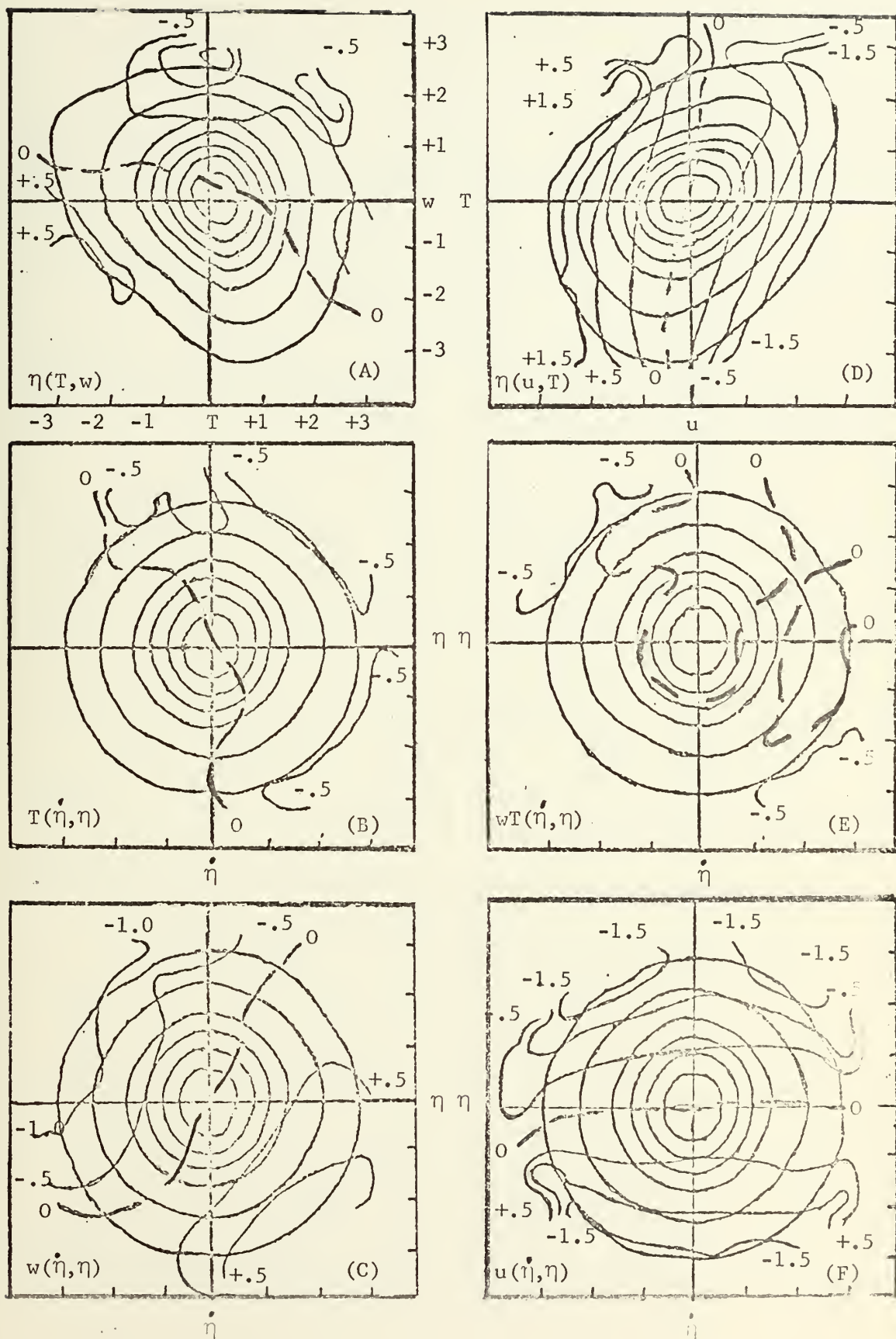


Figure 36. JDF/CMF Results for period 3 subset 2.

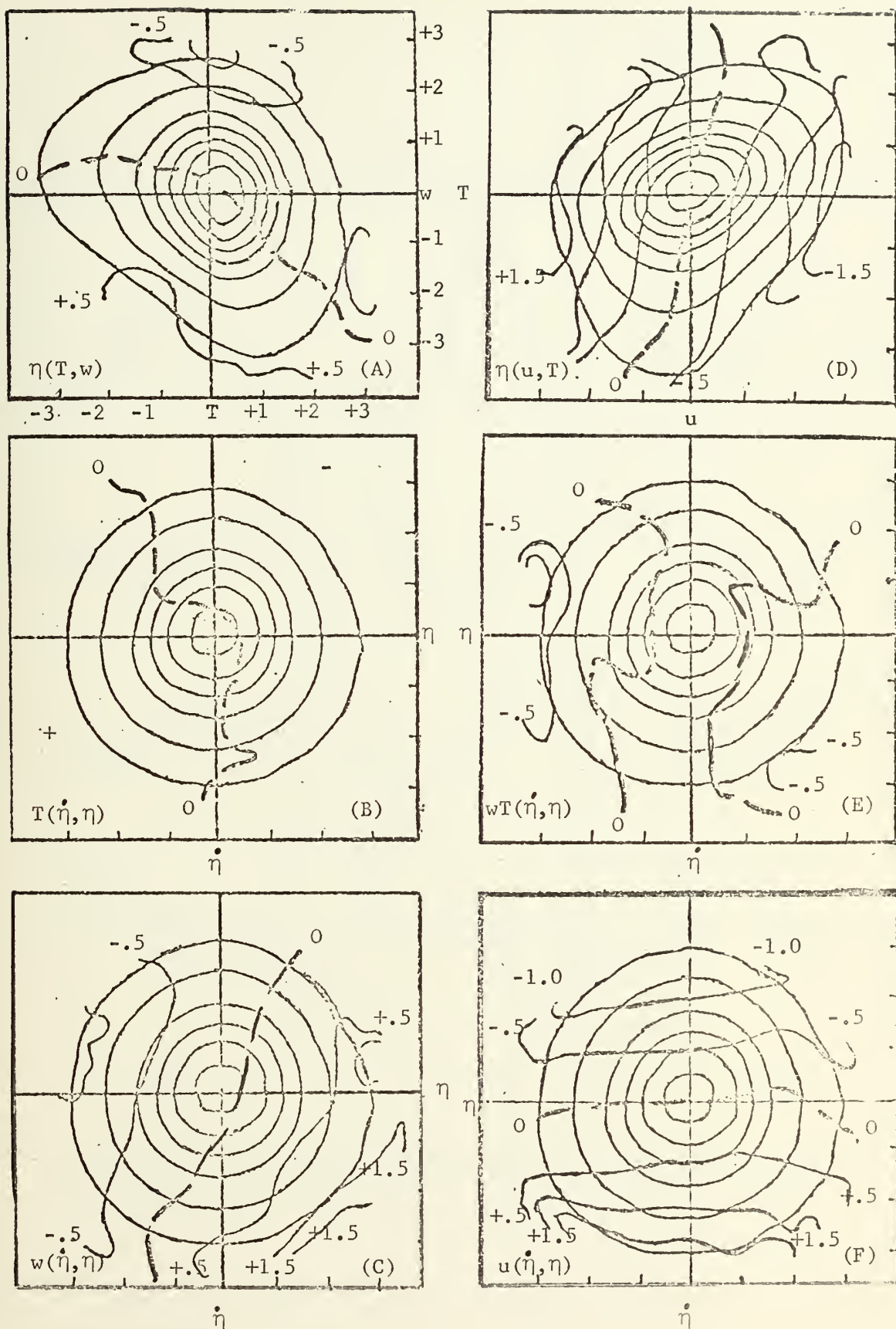


Figure 37. JDF/CMF Results for period 3 subset 3.

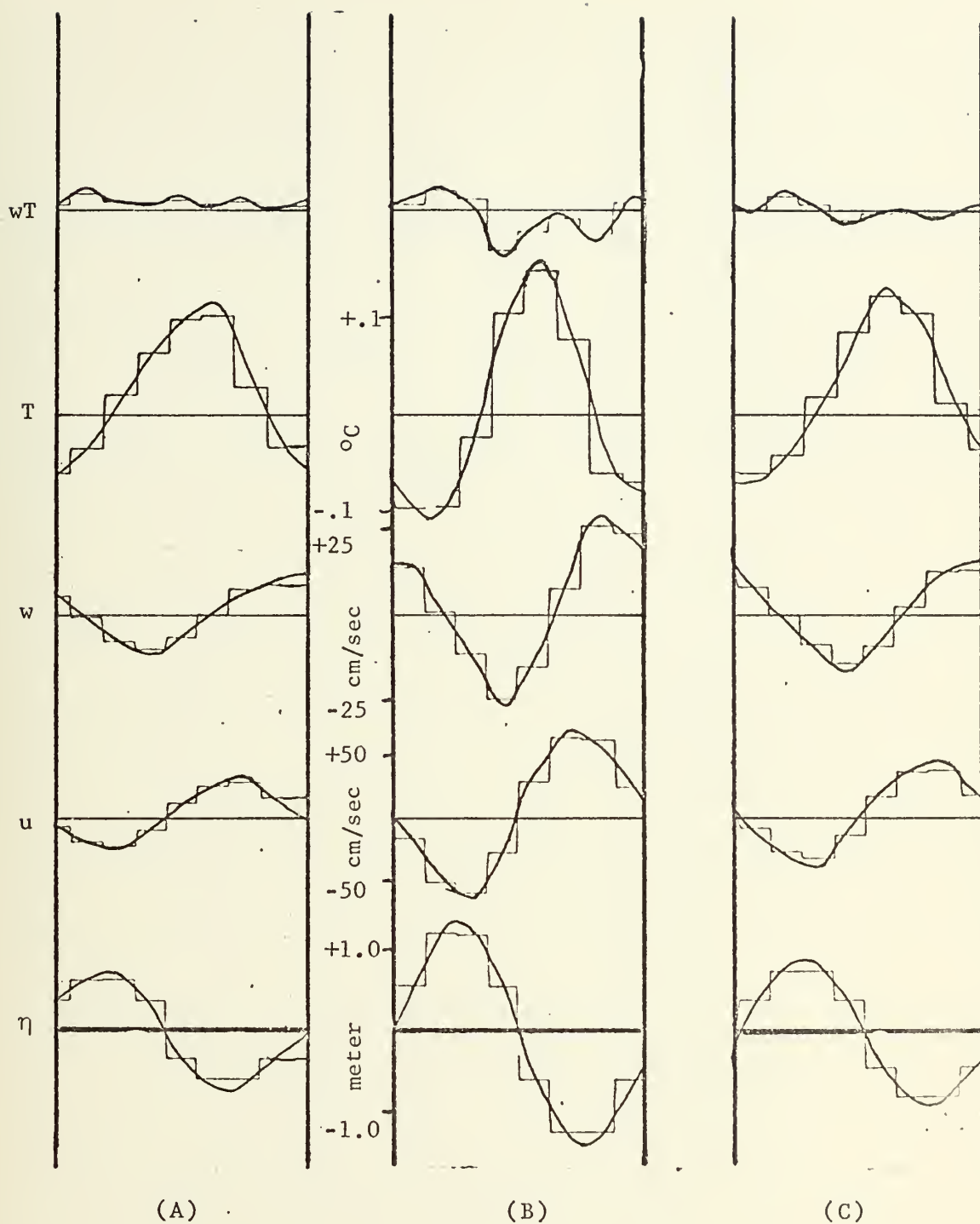


Figure 38. Phase amplitude results for period 3 subset 2 (a) small waves, (b) large waves, and (c) all waves.

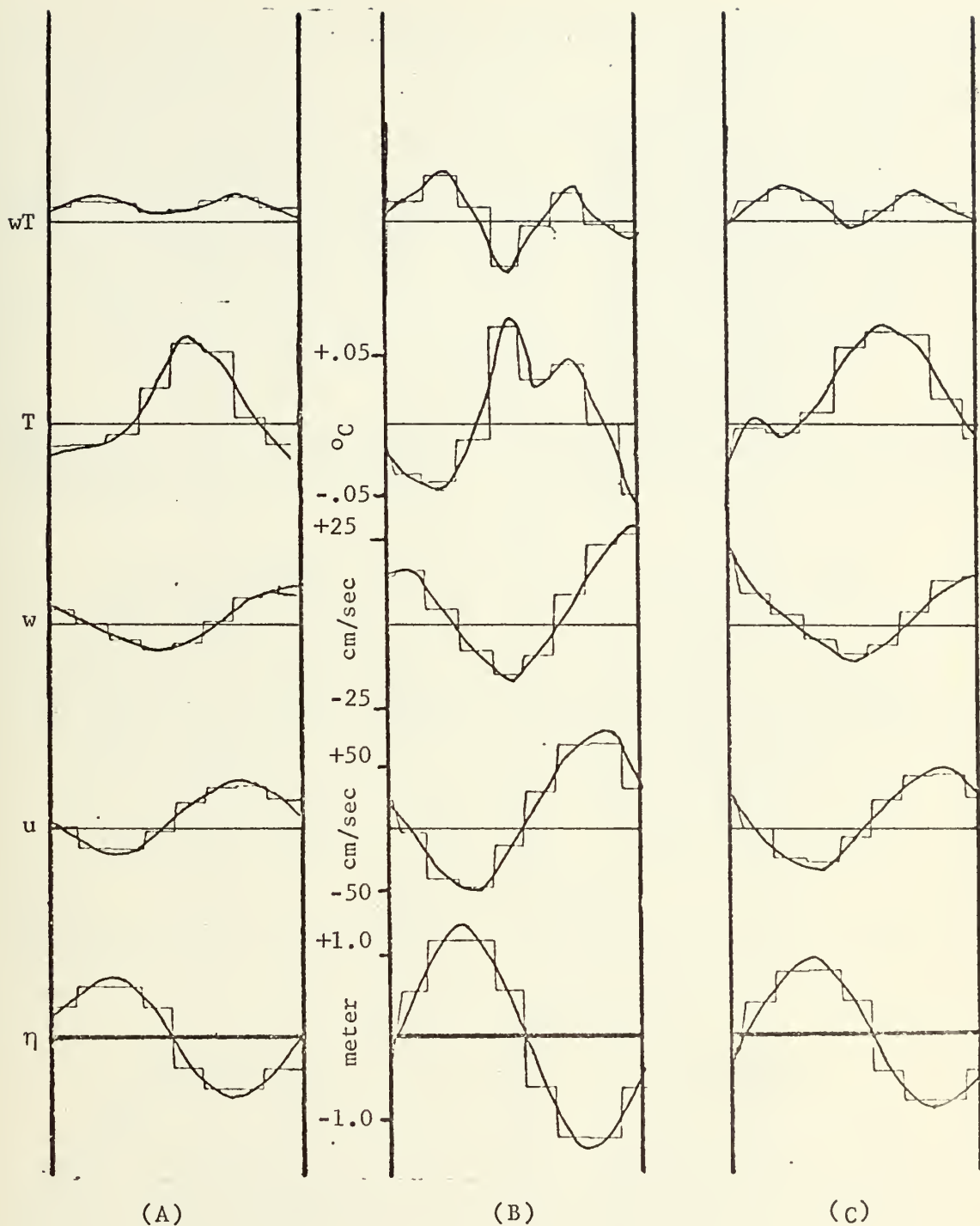


Figure 39. Phase amplitude results for period 3 subset 3 (a) small waves, (b) large waves, and (c) all waves.

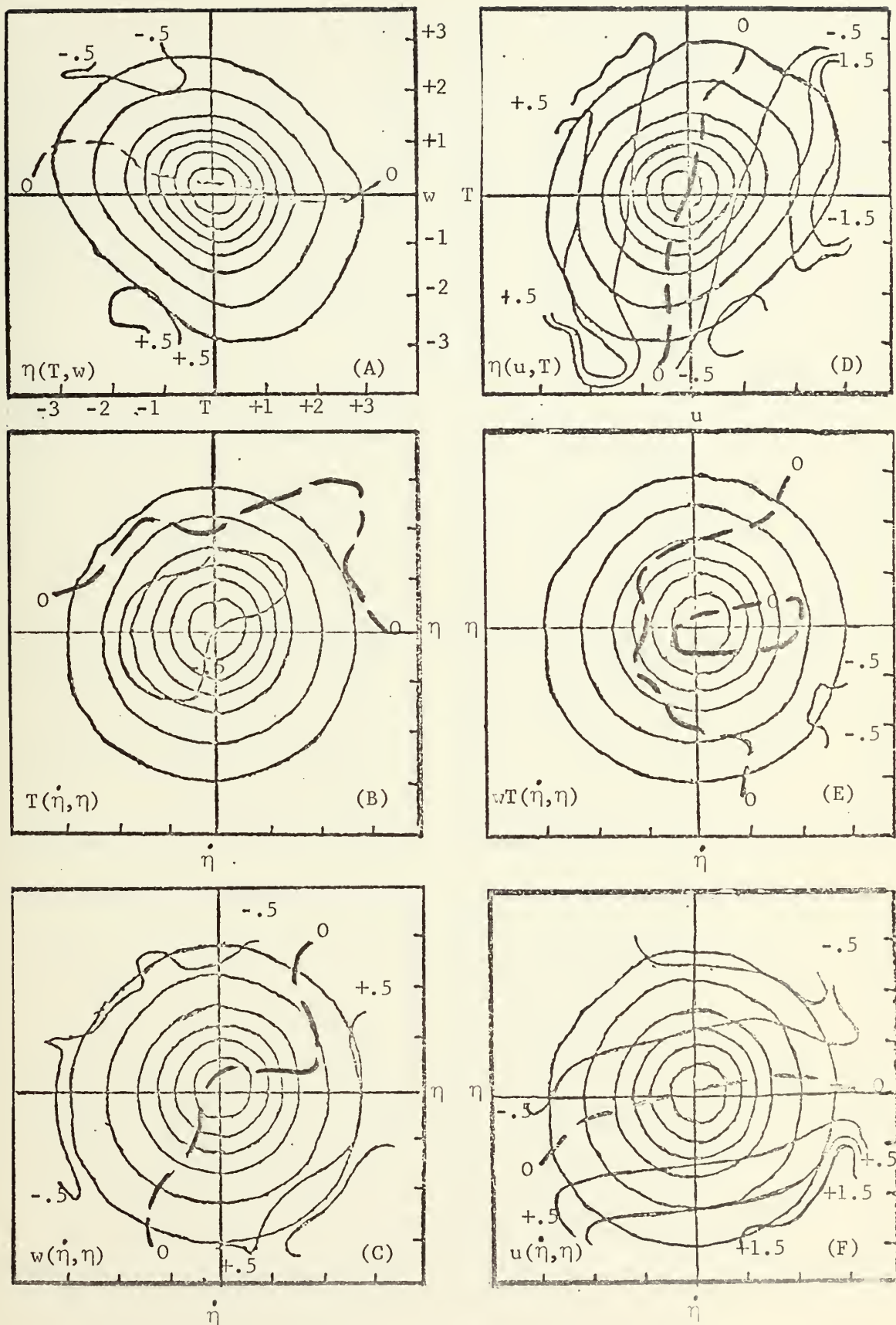


Figure 40. JDF/CMF Results for period 4 subset 2.

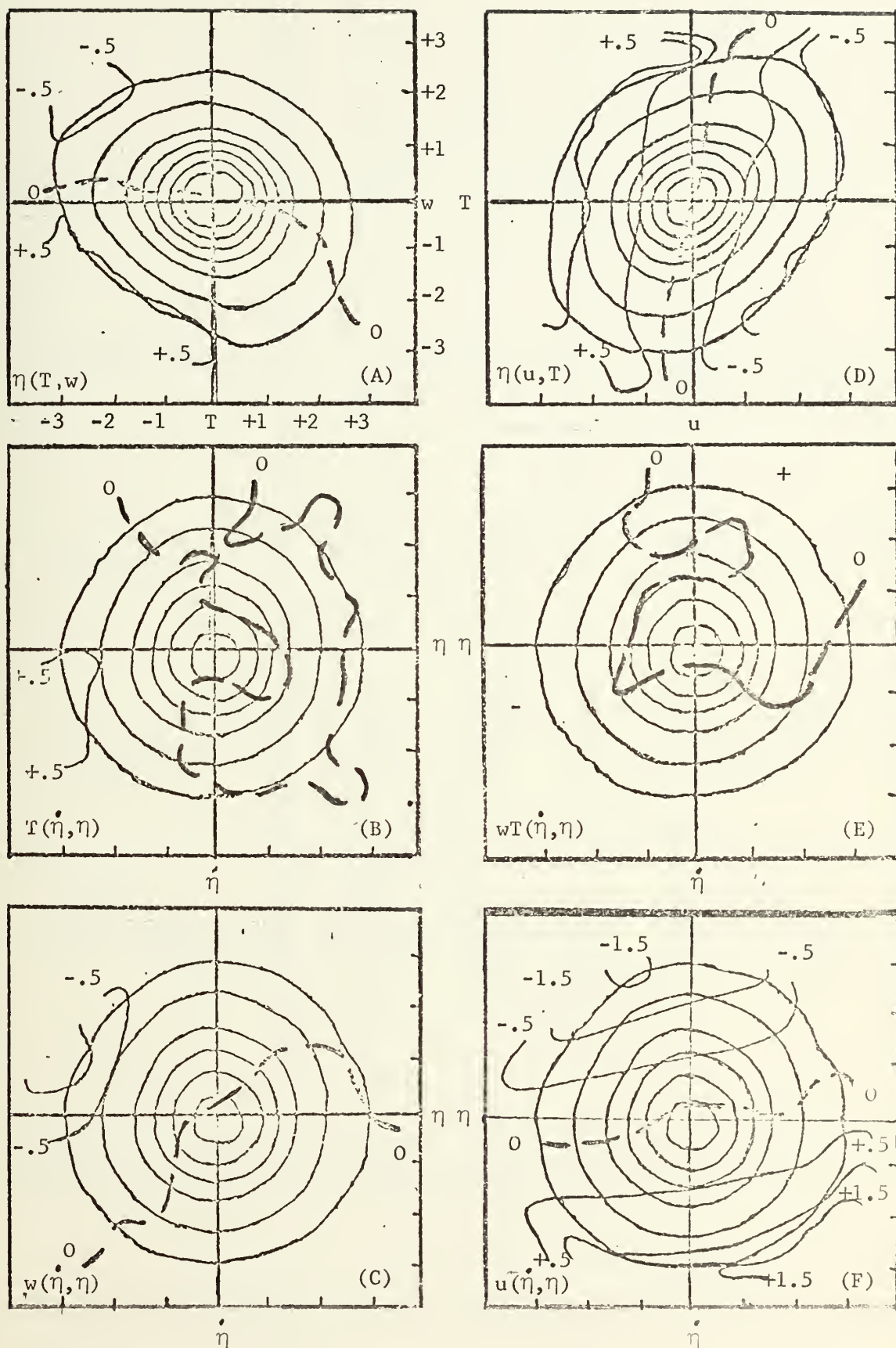


Figure 41. JDF/CMF Results for period 4 subset 3.

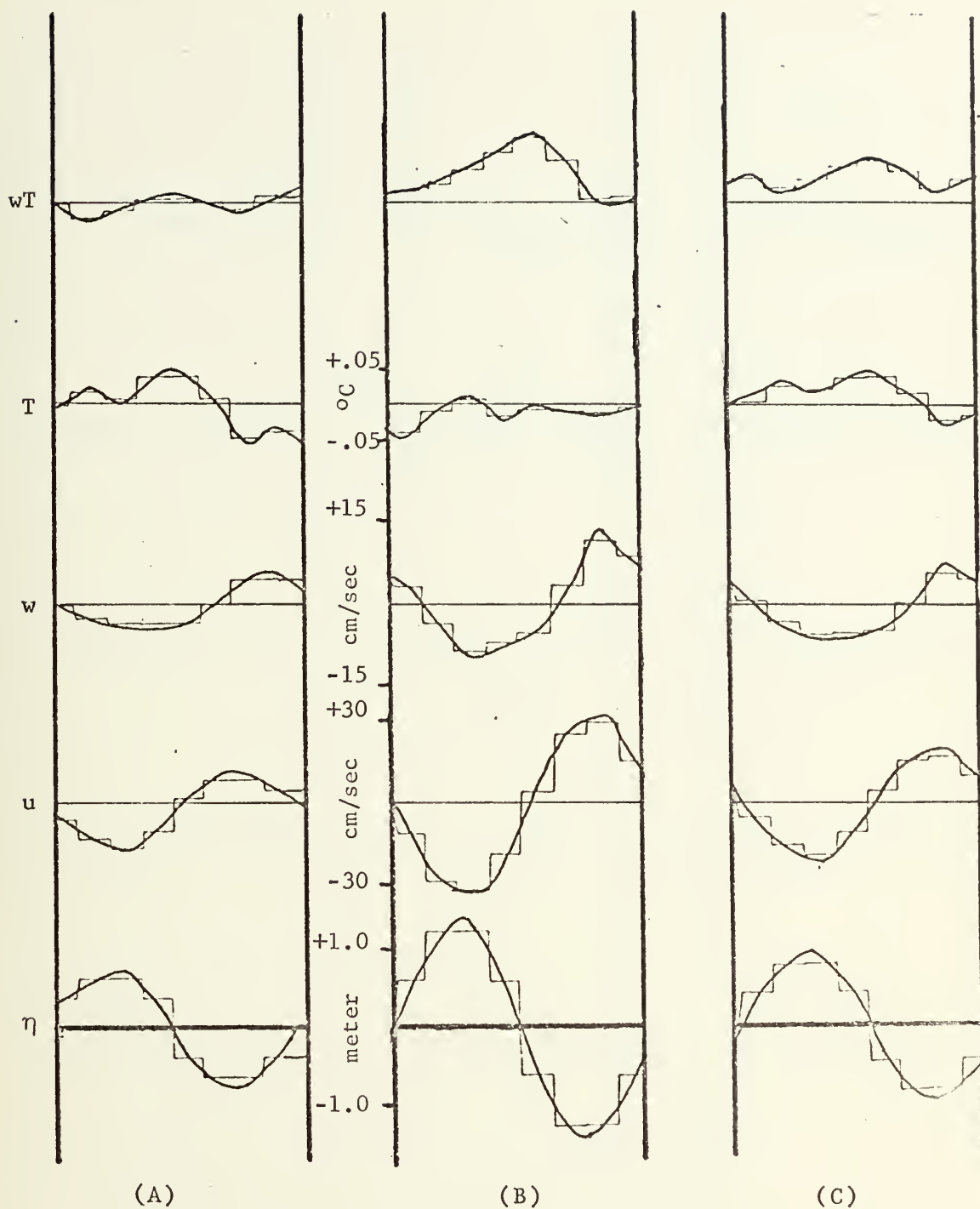


Figure 42. Phase amplitude results for period 4 subset 2 (a) small waves, (b) large waves, and (c) all waves.

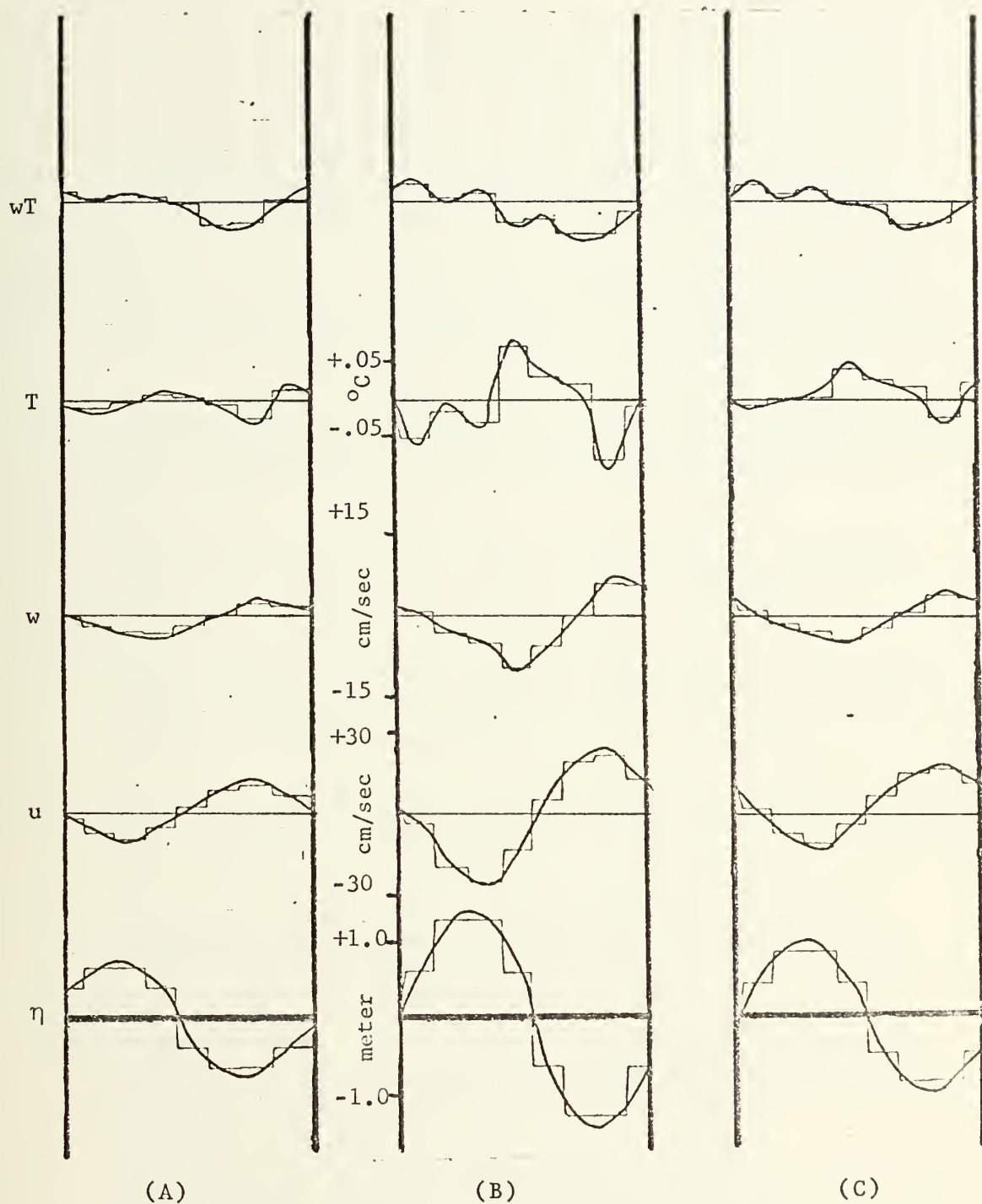


Figure 43. Phase amplitude results for period 4 subset 3
 (a) small waves, (b) large waves, and (c) all waves.

BIBLIOGRAPHY

1. Davidson, K. L., 1970: An investigation of the influence of water waves on the adjacent airflow. ORA Report 08849-2-T. Department of Meteorology and Oceanography, University of Michigan, 259 pp.
2. _____, and A. J. Frank, 1973: Properties of wave-related fluctuations in the airflow above natural waves. J. Phy. Ocean., 3(1) (in press, will appear in Jan. 1973).
3. _____, and G. W. Safley, 1973: Temperature fluctuations and sensible heat transfer above waves. Proc. 15th Conf. on Great Lakes Res., (in press, to appear Feb. 1973).
4. Deacon, E. L., 1959: The measurement of turbulent transfer in the lower atmosphere. Adv. in Geophys., (6).
5. Frank, A. J., 1971: An investigation of the properties and influence of wave induced organized motion in the adjacent airflow. Master's Thesis, Naval Postgraduate School, September 1971. 84 pp.
6. Holland, J. Z., 1968: An application of some statistical technique to the study of eddy structure, TID-24585, U.S. Atomic Energy Commission, Washington, D. C., 378 pp.
7. _____, 1973: A statistical method for analyzing wave snaps and phase relationships of fluctuating geophysical variables. J. Phys. Ocean., 2., (in press, to appear Jan. 1973).
8. Kitaygordskiy, S. A., 1969: Small scale atmosphere-ocean interactions, IVZ, Atmospheric and Oceanic Physics, Academy of Sciences, USSR, 5(11), Eng. Trans. K. Syers, 641-649.
9. Phelps, G. T. and S. Pond, 1971: Spectra of the temperature and humidity fluctuations and the fluxes of moisture and sensible heat in the marine boundary layer. J. Atmos. Sci., 28(6), 918-928.
10. Pond, S., G. T. Phelps, and J. E. Paquin, 1971: Measurements of the turbulent fluxes of momentum, moisture and sensible heat over the ocean. J. Atmos. Sci., 28(6), 901-917.

11. Portman, D. J., K. L. Davidson, and M. A. Walter, 1970: An investigation of the structure of turbulence and of the turbulent fluxes momentum and heat over waves, ONR Tec. Report N00014-67-A-0181-0005, University of Michigan.
12. Stewart, R. H., 1969: Turbulence and waves in a stratified atmosphere. Radio Sci. 4(12), 1269-1278.
13. Thompson, S. P., 1972: Wave-related disturbances in the velocity field over ocean waves, Master's Thesis, Naval Postgraduate School, September 1972, 77 pp.
14. Volkov, Y. A., 1969: The spectra of velocity and temperature fluctuations in airflow above the agitated sea surface, IZV. Atmospheric and Oceanic Physics, Academy of Sciences, USSR, 5(12), Eng. Trans. by J. Findlay, 723-731.
15. Witting, J., 1972: Temperature fluctuations at an air-water interface caused by surface waves. J. Geophy. Res., 77(18), 3265-3269.

INITIAL DISTRIBUTION LIST

	No. Copies
1. Defense Documentation Center Cameron Station Alexandria, Virginia 22314	2
2. Library, Code 0212 Naval Postgraduate School Monterey, California 93940	2
3. Professor Kenneth L. Davidson, Code 51Ds Department of Meteorology Naval Postgraduate School Monterey, California 93940	5
4. Lieutenant David M. Ihle, USN USS CALOOSAATCHEE (A098) FPO New York, New York 09501	2
5. Professor Noel Boston, Code 58Bb Department of Oceanography Naval Postgraduate School Monterey, California 93940	1
6. Professor Edward Thornton, Code 58Tm Department of Oceanography Naval Postgraduate School Monterey, California 93940	1
7. Department of Meteorology, Code 51 Naval Postgraduate School Monterey, California 93940	2
8. Professor G. J. Haltiner, Code 51Ha Department of Meteorology Naval Postgraduate School Monterey, California 93940	1
9. Dr. Donald J. Portman Department of Meteorology and Oceanography University of Michigan Ann Arbor, Michigan 48103	1
10. Commander, Naval Weather Service Command Naval Weather Service Headquarters Washington Navy Yard Washington, D. C. 20390	1

DOCUMENT CONTROL DATA - R & D

(Security classification of title, body of abstract and indexing annotation must be entered when the overall report is classified)

1. ORIGINATING ACTIVITY (Corporate author) Naval Postgraduate School Monterey, California 93940		2a. REPORT SECURITY CLASSIFICATION Unclassified	
		2b. GROUP	
3. REPORT TITLE An Investigation on Temperature Fluctuations over Ocean Waves			
4. DESCRIPTIVE NOTES (Type of report and, inclusive dates) Master's Thesis; September 1972			
5. AUTHOR(S) (First name, middle initial, last name) David M. Ihle			
6. REPORT DATE September 1972		7a. TOTAL NO. OF PAGES 89	7b. NO. OF REFS 15
8a. CONTRACT OR GRANT NO.		9a. ORIGINATOR'S REPORT NUMBER(S)	
b. PROJECT NO.			
c.		9b. OTHER REPORT NO(S) (Any other numbers that may be assigned this report)	
d.			
10. DISTRIBUTION STATEMENT Approved for public release; distribution unlimited.			
11. SUPPLEMENTARY NOTES		12. SPONSORING MILITARY ACTIVITY Naval Postgraduate School Monterey, California 93940	
13. ABSTRACT <p>Joint probability distributions and conditional means functions are used to analyze turbulent wind and temperature data obtained over natural ocean waves. The data were collected aboard R/V FLIP during BOMEX 1969.</p> <p>Stable conditions prevailed during all time periods considered. The emphasis is to use the statistical procedures to describe the wave's influence on the temperature fluctuations at the 8 meter level.</p> <p>Results are compared with predictions given by potential flow theory. The results consistently demonstrate that waves exert an influence on the temperature fluctuations. In addition, it is observed that under near neutral thermal stratification or prolonged periods of stable thermal stratification the temperature fluctuations approached those expected from potential flow.</p>			

14. KEY WORDS	LINK A		LINK B		LINK C	
	ROLE	WT	ROLE	WT	ROLE	WT
Turbulence						
Wave-induced motion						
Temperature fluctuations						
Observational data						
Potential flow predictions						
Wind-wave coupling						
BOMEX						
R/V FLIP						

Thesis
I18
c.2

Ihle

138188

An investigation on
temperature fluctuations
over ocean waves.

Thesis
I18
c.2

Ihle

138188

An investigation on
temperature fluctuations
over ocean waves.

thesl18

An investigation on temperature fluctuat



3 2768 002 10217 0

DUDLEY KNOX LIBRARY